

**Application of alteration minerals and thermal fluid geochemistry in
geothermal conceptual modeling, case study of Olkaria geothermal
field in Kenya**

MIBEI GEOFFREY KIPTOO

I56/78011/2009

**A dissertation submitted in partial fulfillment of the requirements for the
degree of Master of Science in Applied Geochemistry**

APRIL, 2012


DECLARATION

I hereby declare that this dissertation is my original work and has not been presented for a degree in any other university or any other award.

Signature  Date: 27/4/2012

Mr. Geoffrey Kiptoo Mibei
University of Nairobi
School of Physical Sciences
Department of Geology

We hereby confirm that Mr. Geoffrey Kiptoo Mibei is candidate under our supervision undertaking the work reported in this dissertation;

Signature  Date: 5/5/2012

Dr. Daniel Olago
University of Nairobi
School of Physical Sciences
Department of Geology

Signature  Date: 5/05/2012

Dr. Christopher Nyamai
University of Nairobi
School of Physical Sciences
Department of Geology

ABSTRACT

The Olkaria geothermal field is located within the central sector of the Kenyan Rift Valley in Naivasha basin. It is a high-temperature geothermal system and is associated with late Quaternary rhyolite volcanism. The surface geology of Olkaria is mainly characterized by comendite lavas, trachyte lavas and pyroclastics while low lying areas are mainly masked by Holocene sediments especially in the Ol'Njorowa Gorge. Shallow rhyolitic intrusions are thought to be the heat source for the geothermal system. This study considers geothermal conceptual modeling as an important tool in exploration and exploitation of geothermal resources. The main objective is to use thermal fluids and hydrothermal alteration mineral geothermometry to develop a conceptual model of the Olkaria geothermal field. Hydrothermal alteration mineralogy and thermal fluid chemistry are important sources of useful information in geothermal conceptual modeling. Alteration minerals can be used to infer subsurface formation temperatures and also reconstruct the thermal history of a geothermal field. Chemical and solute geothermometers from thermal fluid analysis on the other hand help in the calculation of subsurface temperatures. The approach pursued in the study included; (1) The chemical analysis of major elements in the thermal fluids from Olkaria Northeast, Olkaria East and Olkaria Domes subfields, in order to calculate subsurface temperatures using geothermometric equations by Fournier (1979), Arnosson et al. (1983) and Giggenbach (1988). (2) The use of lithological logs from wells OW-710, OW-23 and OW-910A drilled in the aforementioned subfields to reconstruct lithostratigraphy and hydrothermal alteration zonation. The key index minerals are identified and temperature isotherms mapped. The temperature results from thermal fluids and alteration minerals are analyzed and correlated to identify the inflow, upflow and the outflow. The data is analyzed with the help of high definition softwares such as Rockworks, Surfer and ArcGIS. In this study, minerals such as epidote and actinolite are identified, they infer temperatures of $>250^{\circ}\text{C}$ and 280°C respectively and are markers for an upflow zone in the system. Results from calculated temperature on fluid chemistry and inferred temperatures from alteration minerals, indicate an anomalously relatively high subsurface temperature in Olkaria Northeast compared to Olkaria East and Olkaria Domes. This indicates that the Northeast field is one of the upflow zones for the Olkaria geothermal system.

ACKNOWLEDGEMENT

This study was made possible with the assistance of a number of selfless individuals and organizations. I deeply appreciate the assistance and continued guidance I have received from my supervisors, Dr. D. Olago and Dr. C. Nyamai. Dr. Olago relentlessly guided me during the proposal writing, data setup and synthesis and the write-up of the dissertation. Dr. Nyamai patiently supplied me with fruitful criticisms and much-needed inputs that added value to the study. I also appreciate the focused contribution from Dr. Kuria (of University of Nairobi), Mr. John Lagat, Paul Odhiambo and Irene Mboin (of Geothermal Development Company) touching on specific areas of this dissertation especially the field planning. To the Kenya Electricity Generating Company (Kengen) for the help they provided in carrying out field mapping, sample analysis and provision of other relevant data.

I am grateful to the administration of the University of Nairobi for the scholarship they offered me for my MSc. studies. I acknowledge the support and guidance from the entire administration and staff of Geology department under the chairmanship of Dr. C. Nyamai. I specifically express my gratitude to both the teaching staff and technical team in the department for their selfless services. To my colleagues, thank you for your encouragement, helpful data and information you provided for my dissertation. To my family, you gave me the motivation and love that I badly needed during this time. And above all, to God who enabled me to accomplish this hectic though worthy course in sound health.

TABLE OF CONTENTS

DECLARATION	ii
ABSTRACT.....	iii
ACKNOWLEDGEMENT.....	iv
TABLE OF CONTENTS.....	v
CHAPTER ONE	1
1.0 INTRODUCTION.....	1
1.1 Background information	1
1.2 Statement of problem	3
1.3 Objectives.....	3
1.3.1 Main objective	3
1.3.2 Specific objectives.....	3
1.4 Justification and significance	4
1.5 Literature review	4
1.5.1 Lithology	4
1.5.2 Hydrothermal alteration minerals.....	5
1.5.3 Thermal fluid geochemistry.....	8
CHAPTER TWO	11
2.0 THE STUDY AREA.....	11
2.1 General information	11
2.2 Physiography and drainage	12
2.3 Geological setting.....	13
2.3.1 Regional geology.....	13

2.3.2 Local geology	15
2.3.3 Structural geology and tectonics.....	17
2.4 Hydrogeology	19
CHAPTER THREE	21
3.0 METHODOLOGY	21
3.1 Data sourcing and handling.....	22
3.2 Data interpretation.....	22
3.3 Field work	22
3.3 Laboratory methods.....	24
3.3.1 Stereo microscope analysis.....	24
3.3.2 X-ray diffractometer analysis	24
3.3.3 Petrographic microscope analysis	24
CHAPTER FOUR.....	25
4.0 RESULTS.....	25
4.1 Surface geology of Olkaria.	25
4.2 Lithology	28
4.3 Stratigraphic correlation.....	32
4.4 Petrochemistry of Olkaria field rocks.	34
4.5 Description and distribution of hydrothermal alteration minerals	37
4.6 Hydrothermal zonation.....	44
4.7 Fluid geochemistry of the Olkaria fields.....	46
4.8 Solute geothermometry	47
CHAPTER FIVE	49
5.0 DATA SYNTHESIS AND THE CONCEPTUAL MODELLING.....	49
5.1 Geology and petrochemistry	49

5.1.1 Surface geology of Olkaria.....	49
5.1.2 Lithostratigraphy	50
5.1.3 Petrochemistry	50
5.2 Fluid geochemistry and geothermometry.....	51
5.3 Hydrothermal alteration and zonation.....	52
5.4 Conceptual model.....	53
CHAPTER SIX	57
6.0 CONCLUSION AND RECOMMENDATIONS.....	57
6.1 Conclusion.....	57
6.2 Recommendations.	58
REFERENCES.....	58
APPENDIX IA: Preparation of samples for clay analysis	63
APPENDIX IB: A flow chart on procedure for XRD analysis.....	64
APPENDIX II: Well log of OW-912A based on binocular microscope analysis.....	65
APPENDIX III: Clay analysis and interpretation.	78

LIST OF FIGURES

Figure 1.1: Georeferenced Olkaria subfields in UTM coordinates.....	1
Figure 1.2: Cl-SO ₄ -HCO ₃ Ternary diagram.....	9
Figure 2.1: Map of the study area.	11
Figure 2.2: Physiography of around Olkaria geothermal field.....	12
Figure 2.3 : The Great Rift Valley system.	14
Figure 2.4: Quaternary volcanic centers	16
Figure 2.5: Olkaria ring structure.....	18
Figure 2.6: Regional hydrogeological map.....	19
Figure 3.1: A flowchart the five primary stages in the study.....	21
Figure 3.2: Location of study wells.....	23
Figure 4.1: The geological map of Olkaria area.	23
Figure 4.2: Lithology and hydrothermal alteration minerals in well OW-710.	29
Figure 4.3: Lithology and hydrothermal alteration minerals in well OW-912A.....	30
Figure 4.4: Lithology and hydrothermal alteration minerals in well OW-23.	31
Figure 4.5: Geological cross-section between well OW-912A,OW-23 and OW-710.	33
Figure 4.6: TAS Classification based on the petrochemical results.....	36
Figure 4.7: Classification in terms of Al ₂ O ₃ -total iron as FeO diagram	37
Figure 4.8: Diffractogram showing calcite peaks	37
Figure 4.9: Vescicle filling chlorite in thin section	39
Figure 4.10: Diffractograms showing chlorite peaks	40
Figure 4.11: Diffractograms showing illite peaks.....	42
Figure 4.12: Diffractogram showing pyrite peaks	43
Figure 4.13: Distribution of hydrothermal across wells OW-912A, OW-23 and OW-710	45
Figure 4.14: Average chloride concentration from Olkaria fields.	46

Figure 4.15: Temperatures inferred from the K/Na ratios	47
Figure 4.16: Temperatures inferred from the quartz geothermometry.....	48
Figure 5.1: Cross-section line (A, B, C, and D).....	54
Figure 5.2: Integrated conceptual geothermal model.....	55
Figure 5.3: A three dimensional conceptual model of Olkaria geothermal field.....	56

LIST OF TABLES

Table 1.1: Location of wells OW- 23,OW-710 and OW-912A.....	2
Table 1.2: Common alteration minerals with their equilibrium temperatures.....	6
Table 1.3: Common hydrothermal alteration minerals and temperature stability ranges.....	7
Table 1.4: Primary minerals and their altered equivalents.....	8
Table 4.1: Petrochemistry of Olkaria Northeast and East fields.....	34
Table 4.2: Chemistry of Olkaria domes.....	35
Table 5.1: Hydrothermal alteration mineral in the study wells.....	52

CHAPTER ONE

1.0 INTRODUCTION

1.1 Background information

The Olkaria Geothermal field is a high-temperature geothermal system located within the central sector of the Kenyan Rift Valley in Naivasha basin. It is associated with late Quaternary rhyolite volcanism (Omenda 1998). The study area has been divided into seven sub fields these are; Olkaria East, Olkaria Central, Olkaria Northeast, Olkaria West, Olkaria Southwest, Olkaria South, and Olkaria Domes (Figure 1.1).

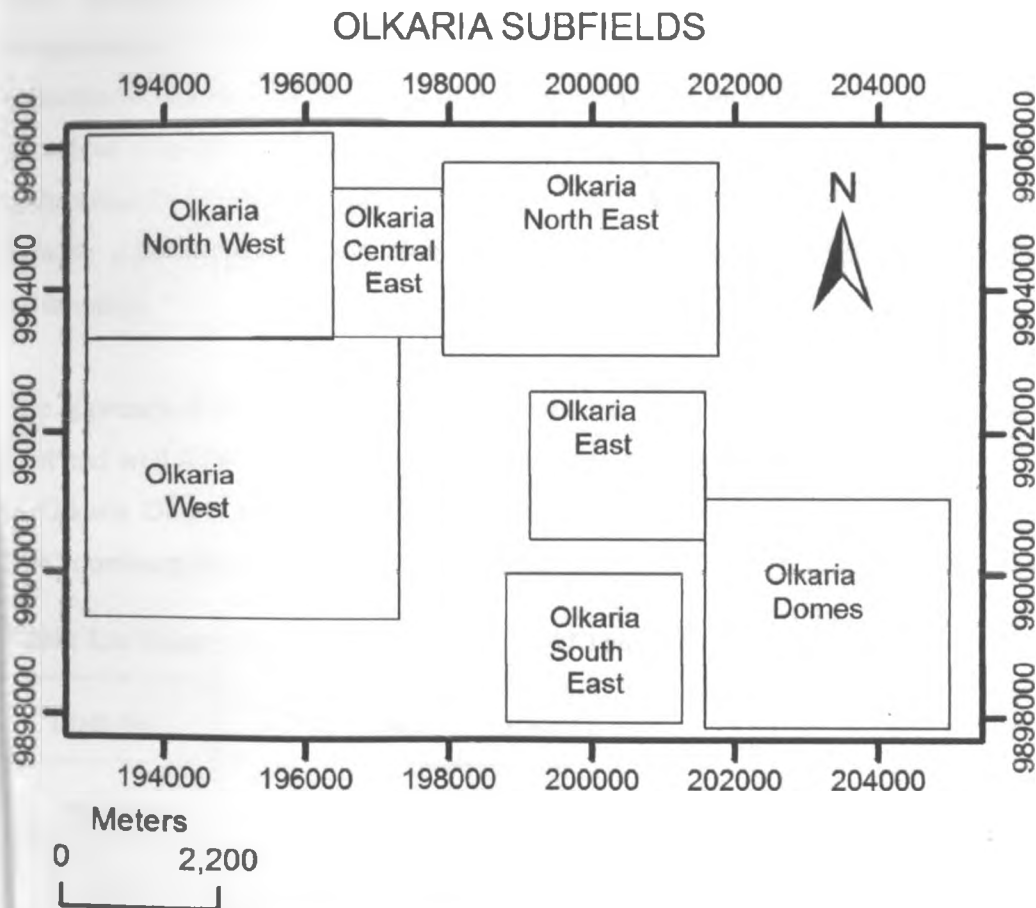


Figure 1.1: Georeferenced Olkaria subfield in UTM coordinates (after Muchemi 2000)

Geothermal resources in this area have been developed since the 1980s. The current installed capacity of about 200 megawatts of electricity and over 110 wells drilled for production and re-injection purposes. Being a high enthalpy geothermal resource with a potential of generating much more steam for electric generation, the current status is far from its full potential. There is therefore a need to invest in drilling of productive wells and increase the electric output. Good production wells can only be achieved by targeting productive areas using an accurately developed model indicating upflow, outflow zones and recharge areas.

This study has helped in understanding the field better and in deriving an accurate model. It describes thermal fluids and hydrothermal alteration minerals geothermometry from Olkaria East, Olkaria Northeast and Olkaria Domes fields. According to Sarolkar (2000), the prominent hydrothermal minerals in geothermal systems are; stilbite, quartz, limonite, smectite, albite with subordinate illite and calcite. Most of these minerals are encountered in Olkaria as hydrothermal alteration minerals. Colin and Patrick (2000) indicated that the success of the application of hydrothermal minerals in geothermometry largely depends on the permeability and ability to achieve equilibrium between fluids and host rocks. Therefore this study is based on this assumption.

The approach of the study is to use data from previous work on well (OW-23) located in Olkaria East and well (OW-710) in Northeast field. Analysis of sample cuttings from well (OW- 912A) in Olkaria Domes using X-Ray diffraction and petrographic methods will also be carried out. The coordinate location in UTM of the mentioned wells are as shown in (Table 1.1) below.

Table 1.1: Location of wells OW- 23, OW-710 and OW-912A (Units in meters)

Well No.	Northing(M)	Easting (M)	Elevations (M)	Depth (M)
912A	9898199	204633	2074	3000
23	9901677	201308	1940	1292
710	9904490	198268	2069	1801

Being an energy deficit country and need to mitigate on the anthropogenic influences on climate change, the Kenya government has opted for geothermal as the best alternative source of energy. Geothermal energy is clean, reliable and independent of erratic climatic patterns. Due to this renewed vigor in geothermal development, drilling of production wells in Olkaria geothermal field is being undertaken by Geothermal Development Company (GDC) under the Ministry of Energy. This study will, therefore be a guide to priority areas for production and possible areas where reinjection wells being drilled by GDC and move closer to realizing the full potential of the Olkaria field.

1.2 Statement of problem

Geothermal resource development has always relied on conceptual modeling and simulations as an approach to understanding a geothermal system comprehensively. Models are imperative in developing strategies of how to efficiently exploit geothermal resources. Alteration minerals and fluid geochemistry can be employed as temperature proxies and consequently guide in pointing out the best drilling targets by indicating possible upflow and outflow zones, recharge areas, as well as permeable zones. A successful study was done in Olkaria Domes (Lagat 2004) using alteration minerals; however, there is need to apply both thermal fluids and alteration mineral characteristics and interaction on a larger scale in various fields. In this regard the study has applied alteration minerals and fluid geochemistry (i.e. chemical geothermometry). This will not only help in developing an integrated geothermal conceptual model of the Olkaria field, but also test the validity and applicability of thermal fluids as temperature proxies.

1.3 Objectives

1.3.1 Main objective

The main objective is to use thermal fluids and hydrothermal alteration mineral geothermometry to develop a conceptual model of the Olkaria geothermal field.

1.3.2 Specific objectives

- Review geology and petrochemistry data of Olkaria geothermal system and relate geological logs from selected wells so as to develop a lithostratigraphic correlation of the area;

- Review fluid chemistry data with respect to solute and chemical geothermometers in order to calculate subsurface temperatures in the field;
- Identify hydrothermal alteration minerals and temperature zonation from sample cuttings in order to infer the subsurface temperatures in each well; and
- Develop a conceptual geothermal model.

1.4 Justification and significance

A conceptual model of Olkaria Domes was developed based on alteration minerals from wells OW-901, OW-902 and OW-903 (Lagat 2004). The model was very instrumental in understanding temperature zonation and locating high value targets in Olkaria Domes area for drilling. The Olkaria geothermal system is, however, large and complex hence understanding it in a detailed manner is important, particularly now when appraisal and production drilling is being scaled up in Olkaria Northeast and East fields which are remote from the better understood Olkaria Domes. This study is of great significance in that it will assess three wells in Olkaria North East, Olkaria East and Domes area by applying alteration mineral characteristics in addition to fluid chemistry data. The results will give more detail information on subsurface temperatures hence elucidating the upflow, outflow and permeable zones in the Olkaria subfields. The ultimate goal is to developing a conceptual model of the three Olkaria sub fields, which will greatly enhance the understanding of the geothermal system. The study will also help validate thermal fluids as proxies in geothermal modeling. The model will be used as a tool for the current and future designs for sustainable exploitation of the resource.

1.5 Literature review

1.5.1 Lithology

Studies by Thomson and Dodson (1963) showed that the surface geology of Olkaria volcanic complex is dominated by pyroclastics which blanket all the other rocks. These pyroclastics were found to be of Quaternary age mainly from Longonot and other small eruption centers within Olkaria. Other lithologic units like the comendites are found in the central parts of Olkaria.

Omenda (1998), Muchemı (2000) and Lagat (2004) working in Olkaria on 90 wells that had been drilled in the field found out that the lithostratigraphic units encountered include pyroclastics,

tuffs, rhyolites, trachyte, phonolites, basalts and minor intrusives. Studies by Lagat (2004) mainly focusing on Olkaria Domes field showed that from the surface to about 400 m below the surface, the predominant lithological units were the pyroclastics. The major lithological units below 400 m were trachyte, basalts with rhyolites and tuffs occurring as intercalations.

1.5.2 Hydrothermal alteration minerals

Extensive research and studies by Browne (1978) and Utami *et al.* (2005) have been done on Olkaria and Indonesian geothermal systems. The results indicated that the chemical composition of host rocks and possible fugitive components from presumed magmatic heat sources determines the availability of components to form hydrothermal alteration minerals. The most critical factor, however, for hydrothermal alteration is temperature because most mineral components are unstable at elevated temperature.

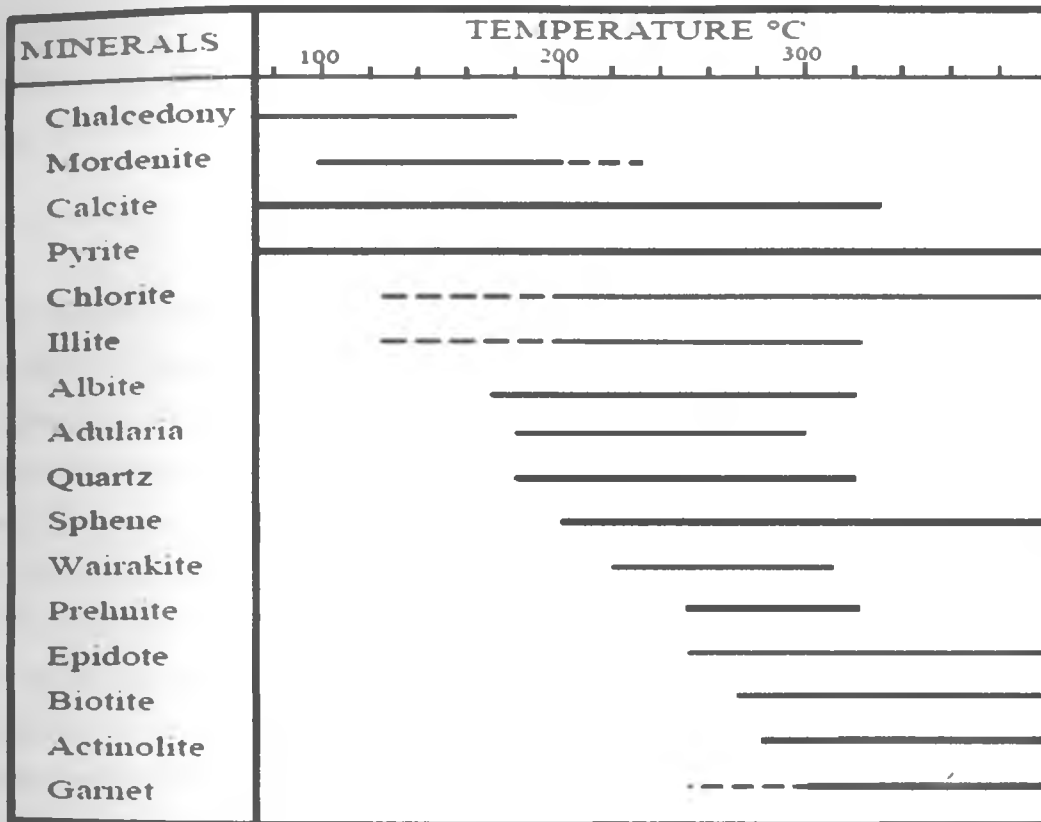
Pressures at depth in the Olkaria wells, like others elsewhere around the world (Browne 1978) are not sufficient to greatly affect hydrothermal alteration of minerals. Therefore temperature and chemistry of host rocks are the critical parameters for hydrothermal alteration in Olkaria fields. Permeability however, has also been found to have a direct bearing on hydrothermal alteration. For example, Colin and Patrick (2000) working in the Philippines geothermal fields showed that permeability of rocks controls the circulation of thermal fluids thus causing hydrothermal alteration and precipitation of secondary minerals in open spaces or fractures. Hydrothermal alteration minerals encountered in Olkaria geothermal field are zeolites at shallow depths while clays, epidote and actinolite are encountered deeper. Table 1.2 below gives various alteration minerals, their chemical formulas and temperatures they infer.

Table 1.2: Common alteration minerals with their equilibrium temperatures (Utami *et al.* 2005)

ALTERATION MINERALS	CHEMICAL FORMULAE	TEMPERATURES IN °C
Zeolite	$K_6[(Al, Si) O_4]$	100-210
Clay	$Al_2O_3 \cdot 2SiO_2 \cdot 2H_2O$	200-300
Actinolite	$Ca_2(Mg, Fe)_5Si_8O_{22}(OH)_2$	>290
Hematite	Fe_2O_3	all environments
Pyrite	FeS_2	all environments
Albite	$NaAlSi_3O_8$	170-310
Titanite (Sphene)	$CaTiSiO_5$	>200
Epidote	$Ca_2(Al, Fe)_3(SiO_4)_3(OH)$	>240
Prenhite	$Ca_2 Al_2 Si_3 O_{10}(OH)_2$	210-310
Wairakite	$CaAl_2Si_4O_{12} \cdot 2(H_2O)$	200-310
Adularia	$KAlSi_3O_8$	190-290

Reyes (1990) while studying the Philippines systems came up with a standard reference chart (Table 1.3) of hydrothermal alteration minerals and the temperatures they infer.

Table 1.3: Common hydrothermal alteration minerals and their temperature stability ranges (after Reyes 1990) (Broken lines indicate minerals outside their usual stability ranges)



A summary of hydrothermal alteration minerals and their primary phases have been postulated by Reyes (1990). From her hypotheses, most of the high temperature index minerals are alteration products of olivine, pyroxene and plagioclases (Table 1.4).

Table 1.4: Primary minerals and their altered equivalents (After Reyes 1990)

Primary phases	Alteration products
Volcanic glass	Zeolites, clays, quartz, calcite
Olivine	Chlorite, actinolite, hematite, clay minerals
Pyroxene, amphiboles	Chlorite, illite, quartz, pyrite, calcite
Ca-plagioclase	Calcite, albite, adularia, quartz, illite, epidote,
Sanidine, orthoclase, microcline	Sphene
Magnetite	Adularia
	Pyrite, sphene, hematite

1.5.3 Thermal fluids geochemistry

An often-used application of thermal fluid geochemical analysis is the calculation of subsurface temperatures using geothermometric equations. Several types of these geothermometers have been studied and described in detail by Karingithi and Wambugu (1997). The basic assumption underlying most geothermometers in fluid chemistry are that the ascent of deeper, hotter waters and the accompanying cooling is fast enough such that kinetic factors will inhibit re-equilibration of the water and minimal mixing with alternate water sources occurs during its ascent. It should be noted that compliance with these assumptions is often exceedingly difficult to prove (Ferguson *et al.* 2009). An additional assumption presented by Fournier (1997) is that all reactants are present in sufficient quantities and that equilibrium itself is attained at depth.

Fluid geothermometry requires a high level of characterization of thermal fluids before their application. The Cl-SO₄-HCO₃ ternary diagram (Figure 1.2) is an important tool in characterization and classification of natural waters (Giggenbach 1991). The position of the data point in such a triangular plot is obtained by evaluating the concentration (in mg/kg) of all three constituents involved.

In the ternary diagram, composition ranges are indicated for several typical groups of water such as volcanic and steam heated waters, mature waters and peripheral waters. From characterization it has been noted chloride waters with near neutral pH are the most reliable indication of deep reservoir temperatures whereas superficial acid sulphate waters give only indication of surficial conditions (Wambugu 1995).

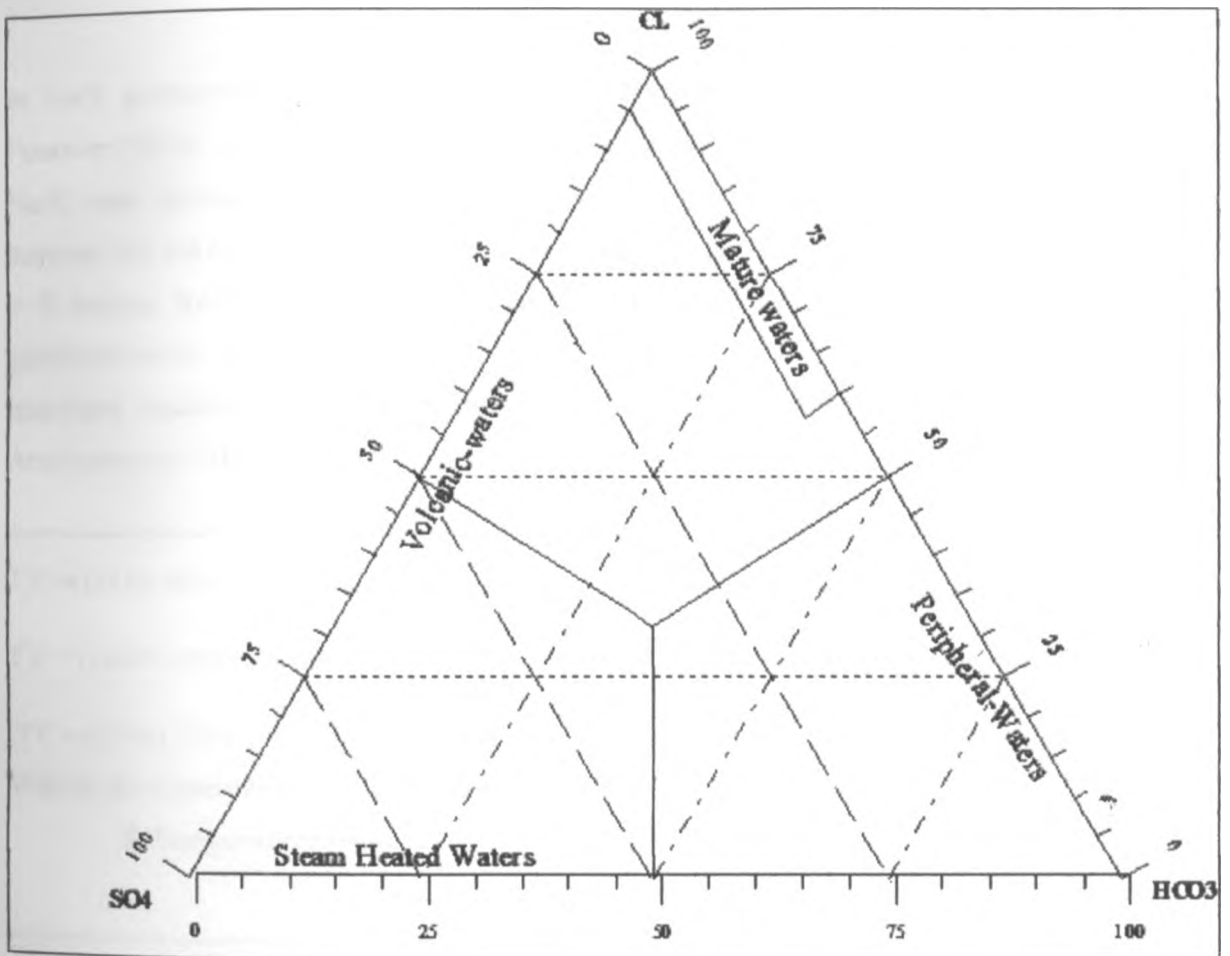


Figure 1.2: Cl-SO₄-HCO₃ Ternary diagram (Modified from Arnorsson *et al.* 1983)

In silica geothermometry, deep fluids with temperatures $>180^{\circ}\text{C}$ are in equilibrium depending on the degree of initial saturation. Below 100°C a solution may remain supersaturated with

respect to silica, the basic equation for silica dissolution being; $\text{SiO}_2(\text{s}) + 2\text{H}_2\text{O} = \text{H}_2\text{SiO}_4$. According to Fournier and Potter (1982) we apply the equation;

$$T^{\circ}\text{C} = -42.198 + 0.2883\text{C} - 3.6686 \times 10^{-4} \text{C}^2 + 3.166 \times 10^{-7} \text{C}^3 + 77.034 \text{Log C} \dots \text{Equation 1}$$

Where: C- Concentration (mg/kg)

T-Temperature(°C)

In Na/K geothermometry, many equations have been developed over the years, for example Fournier (1979), Arnorsson *et al.* (1983) and Giggenbach (1988). The observed response of the Na/K ratio decrease with increase in fluid temperature is due to cation exchange reaction between Na and K bearing feldspars. The equation for such reaction is $\text{K}^+ + \text{Na bearing feldspar} = \text{K-bearing feldspar} + \text{Na}^+$. Waters from high reservoirs temperatures are suitable for this geothermometry with adularia being a very important mineral for this application. The most important equations for Na/K geothermometers have been described by Fournier (1979), Arnorsson *et al.* (1983) and Giggenbach (1988) as;

$$T^{\circ}\text{C} = (1217/1.483) + \log (\text{Na/K}) - 273.15 \dots \text{Equation 2 (Fournier 1979)}$$

$$T^{\circ}\text{C} = (1319/1.699) + \log (\text{Na/K}) - 273.15 \dots \text{Equation 3 (Arnorsson et al. 1983)}$$

$$T^{\circ}\text{C} = (1390/1.750) + \log (\text{Na/K}) - 273 \dots \text{Equation 4 (Giggenbach 1988)}$$

Where: C- Concentration (mg/kg)

T-Temperature (°C)

CHAPTER TWO

2.0 THE STUDY AREA

2.1 General information

The Olkaria geothermal field is situated within Hells Gate National Park in Naivasha, the geographical positioning places the study area between longitudes $36^{\circ}00' E$ and $36^{\circ}30' E$ and latitudes $0^{\circ}30' S$ and $1^{\circ}00' S$. It is southwest of Lake Naivasha and in the southern segment of the Kenya Rift Valley (Figure 2.1). The geothermal field is divided into seven subfields and has a total area of about 140 km^2 .

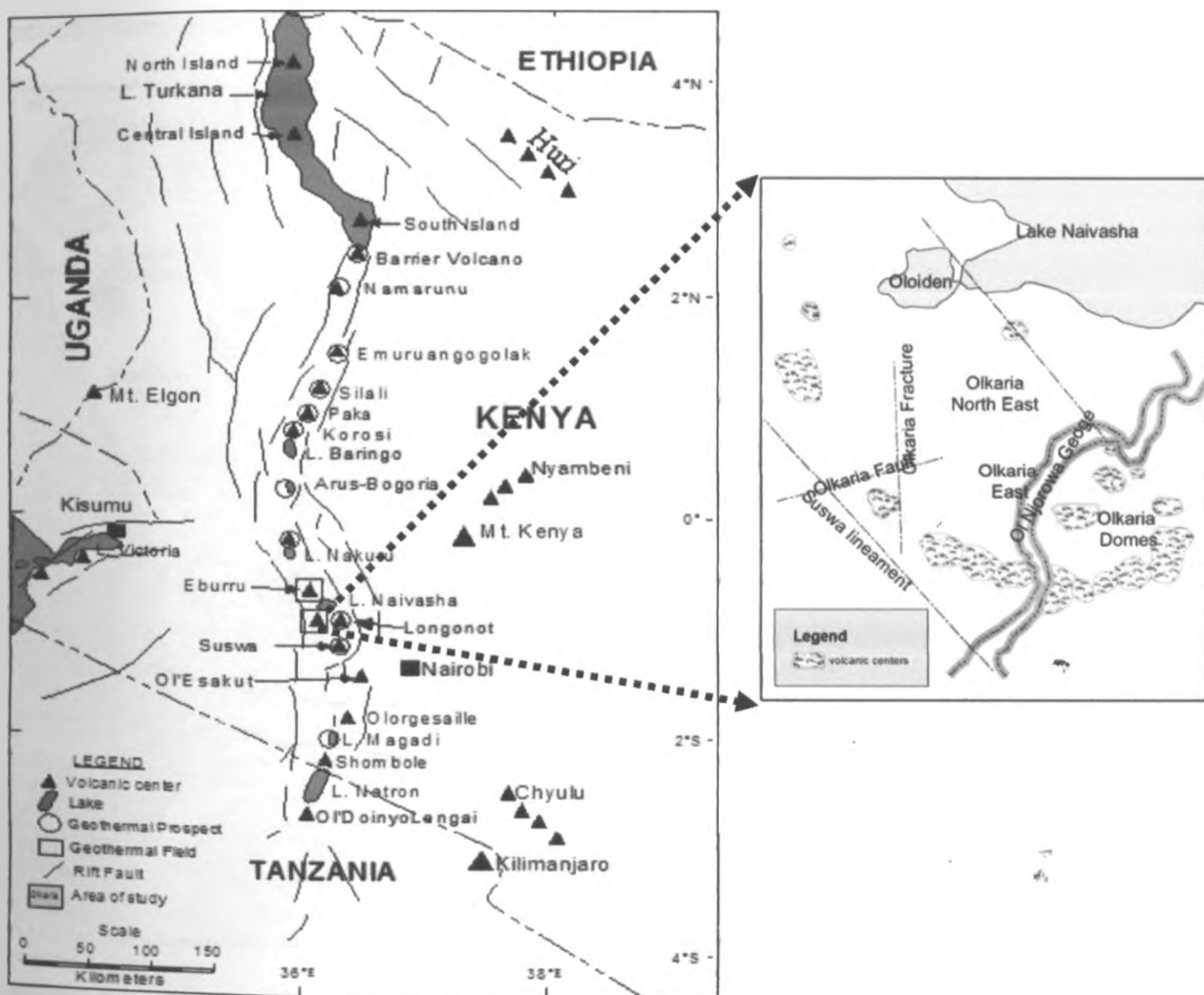


Figure 2.1: Map of the study area

2.2 Physiography and drainage

The physiography of Olkaria geothermal field is impressive; various volcanic masses and scarps formed by both faulting and erosion have created wonderful scenery. The field is flanked to the east and south by Longonot and Suswa caldera volcanoes respectively and to the north is the Eburru pantelleritic dome (Figure 2.2). Lake Naivasha is also an important geographical feature in the northeast at an altitude of 1884m above sea level and an area of about 139 km². There is a general lack of deep dissection within the Olkaria Domes area but to the south is the prominent Ol'Njorowa Gorge. The Gorge is steep sided and 200 m wide with a gently dipping floor to the south. It was an outlet of the lake Naivasha during the lower and middle Gamblian period (Thomson and Dodson 1963).

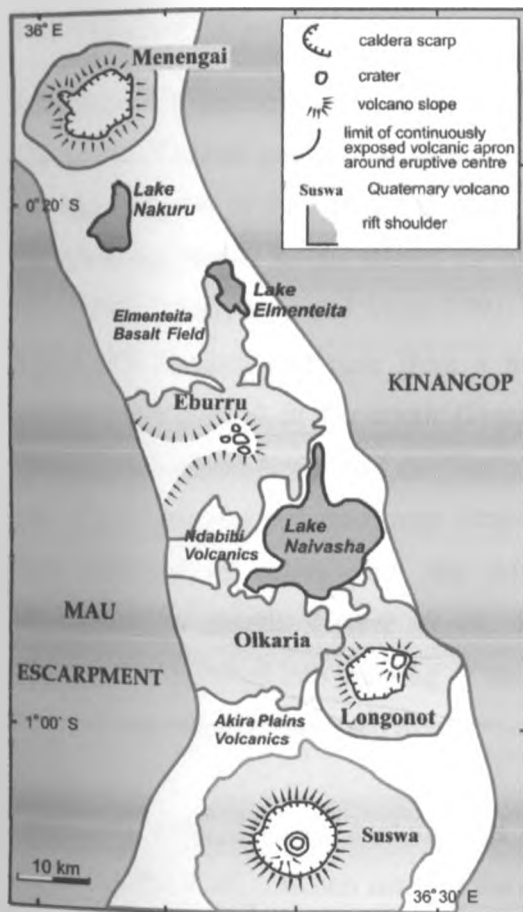


Figure 2.2: Physiography of Olkaria geothermal field (Adapted from Macdonald *et al.* - 2011)

On a regional scale Kinangop Plateau and Mau Escarpment are important controls on the drainage pattern. The Kinangop Plateau is on the northeastern part situated between Aberdare Ranges and the Rift floor. It is a broad flat plain with an altitude of about 2440 m above sea level. The Plateau is deeply incised by Makungi, Kitiri and Engare Magutyu which forms part of Malewa, the largest river flowing to Lake Naivasha (Thomson and Dodson 1963).

The Mau Escarpment with an elevation of approximately 3050 m above sea level forms the western wall of the Rift Valley. It is composed of soft volcanic ashes and tuffs with rare outcrops of agglomerates and lavas. Eburru volcano is linked to the Mau Escarpment by a ridge with an elevation of 2800m above sea level caused by piling up of the pyroclastics. Like the escarpment, the ridge is deeply incised by water courses.

2.3 Geological setting

2.3.1 Regional geology

The greater Olkaria geothermal system is located south of Lake Naivasha, on the floor of the southern segment of the Kenya Rift Valley within the African Rift System. The development of the rift valley within Kenya started during the late Oligocene 3 Million years ago (Baker *et al.* 1971, 1972; Kampunzu and Mohr 1991; Smith 1994). The Kenyan Rift is part of the Eastern Africa Rift System that runs from a triple junction at the Gulf of Aden in the north to Mozambique (Beira) in the south (Figure 2.3). The Kenya Rift Valley extends from Lake Turkana in northern Kenya to Lake Natron in northern Tanzania. This mega tectonic structure is part of a continental divergent zone where dynamic spreading occurred. The rifting process has been modeled as active with the driving force being provided by convection in the asthenospheric mantle (Baker *et al.* 1972; Ambusso and Ouma 1991). The spreading phenomenon resulted into thinning of the crust and is associated with several episodes of lava eruption and other volcanic activities.

Structures controlled the evolution of the eastern Africa rift system, with the rift faults exploiting the weak collision zones at the contact between the Archean Tanzanian craton and the Proterozoic Orogenic belt (Smith and Mosley 1993). Volcanism associated with this rifting started during the Miocene period. This magmatic activity was accompanied by dome uplift of about 300m resulting in eruption of phonolites (Baker and Wohlenberg 1971).

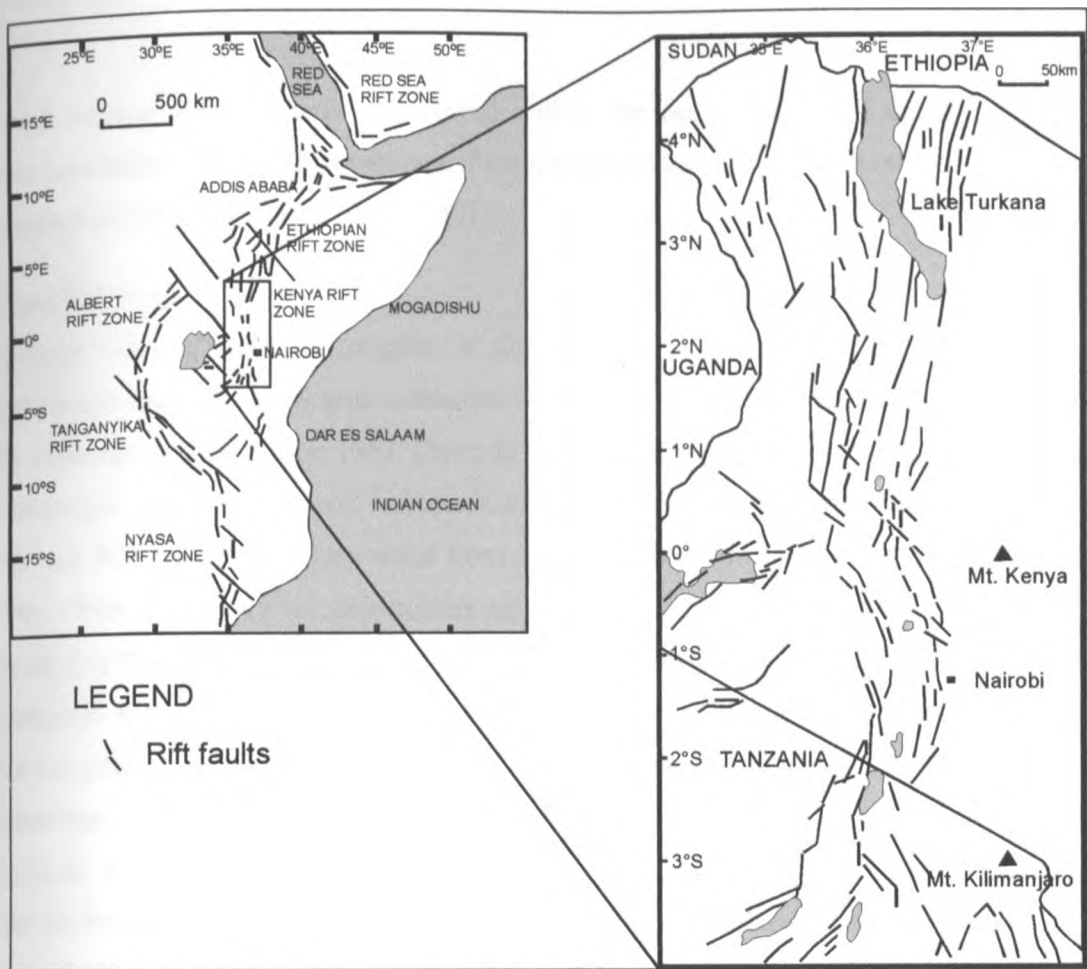


Figure 2.3: The Great Rift Valley system (Modified from Dunkley *et al.* 1993)

The evolution of the rift was sequential with massive and extensive Pliocene eruption of trachytic ignimbrites in the central area, forming the Mau and Kinangop tuffs and was followed by block faulting. A second faulting episode, which followed the ignimbrite eruptions, resulted in the formation of the graben structure as known today. A graben is a long structure compared to its width that is lower relative to the blocks on either side (Billings 1972). In the developing graben, fissure eruptions of trachyte, basalt, basaltic trachy-andesite and trachy-andesite occurred (Baker *et al.* 1971). The plateau rocks that filled the developing graben were then block faulted to create high angle normal faults within the rift floor. The fractures apparently served as conduits for the Quaternary volcanic activity of mafic to felsic composition.

The most intense volcanic activity occurred within the central sector of the rift where the volcanic succession is 5 km thick (estimated from seismic data and information from geothermal wells drilled in Olkaria) (Simiyu *et al.* 1995).

2.3.2 Local geology

The greater Olkaria volcanic complex is characterized by numerous volcanic centers of Quaternary age and is the only area within the Kenya rift with occurrences of comendite on the surface (Thompson and Dodson 1963; Omenda 2000). Magmatic activity in Olkaria occurred in the Pleistocene age and continued to Recent as indicated by the Ololbotut comendite dated at 180 ± 50 year B.P, using carbonized wood from a pumice flow associated with the lava (Clarke *et al.* 1990). Other Quaternary volcanic centers adjacent to Olkaria include Longonot volcano to the southwest and Eburru volcanic complex to the north (Figure 2.4). Whereas the other volcanoes are associated with calderas of varying sizes, Olkaria volcanic complex does not have any clear caldera association. However the presence of a ring of volcanic domes in the east, south, and southwest has been used to invoke the presence of a buried caldera (Naylor 1972; Virkir 1980; Clarke *et al.* 1990). Seismic wave attenuation studies for the whole of the Olkaria area also indicate an anomaly in the area coinciding with the proposed caldera (Simiyu *et al.* 1998). The geology of Olkaria is dominated by Pliocene-Holocene comendite rhyolite flows, basalt, trachyte and tuff (Omenda 1998). The Mau tuffs are the oldest rocks that crop out in the Olkaria area. These rocks are common in the area west of Olkaria Hill, but are absent in the east due to an east dipping high angle normal fault that passes through Olkaria Hill (Omenda 2000).



Figure 2.4: Quaternary volcanic centers (Modified after Muchemi 2000)

Data from lithological logs of earlier drilled wells indicates that there is a basalt (Olkaria basalt), underlying the Upper Olkaria volcanics in the area to the east of Olkaria Hill. This lithological unit, however, is not encountered in the wells drilled in Olkaria West field. The formation varies in thickness from 100 m to 500 m. The surface geology is mainly comendite lavas and their

pyroclastic equivalents, ashes from Suswa and Longonot volcanoes with minor trachytes and basalts (Thompson and Dodson 1963, Ogoso-Odongo 1986, Omenda 2000).

2.3.3 Structural geology and tectonics

Structures in the Greater Olkaria volcanic complex include; the Olkaria fault, Gorge Farm faults, Suswa lineament, and the Ol’Njorowa Gorge (Figure 2.5). The faults are prominent in the Olkaria Central and Olkaria West fields but are scarce in the Olkaria Domes area, possibly due to the thick pyroclastic cover (Ndombi 1981, Omenda 1998). The NW-SE and WNW-ESE faults are thought to be the oldest and are associated with the development of the main Rift Valley. The Gorge Farm fault in the northeastern part extends to Olkaria Domes area and displaces the Ol’Njorowa Gorge in strike slip orientation. The most recent structures in the area are the N-S faults. Hydroclastic craters located on the northern edge of the Olkaria Domes area mark magmatic explosions, which occurred in a submerged terrain. These craters form a row along where the extrapolated caldera rim trace passes.

STRUCTURAL MAP OF OLKARIA

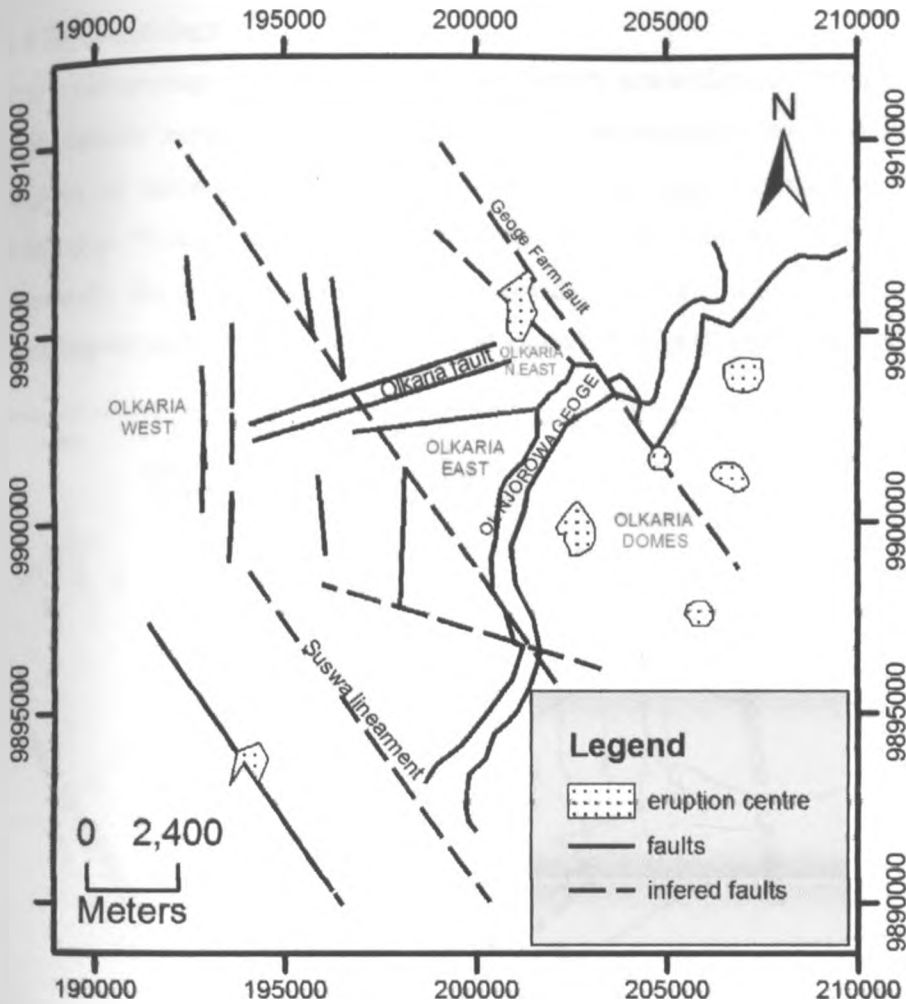


Figure 2.5: Olkaria ring structure (Modified from Clarke *et al.* 1990)

Dyke swarms exposed by the Ol'Njorowa Gorge trend in a NNE direction further attesting to the recent reactivation of faults with that trend. The Ol'Njorowa Gorge was thought to have been formed by faulting but the feature is known today to have been as a result of a catastrophic outflow of Lake Naivasha during its high stands (Clarke *et al.* 1990). Volcanic plugs (necks) and felsic dikes occurring along the Gorge further attests to the fault control in the development of this feature. Subsurface faults have also been encountered in most Olkaria wells (Karingithi 1996).

2.4 Hydrogeology

The hydrogeology of Olkaria area is significantly controlled by tectonics, topography, geology and climatic aspects. Recent tectonic activity has modified the fracture patterns and created regions of enhanced permeability enabling mainly meteoric recharge into the system. The Kinangop Plateau and Mau Escarpments are high altitude areas with high precipitation, especially the Mau Escarpment. This provides meteoric water and hydrogeological gradient enabling an axial flow towards the Rift floor and Olkaria (Figure 2.6).

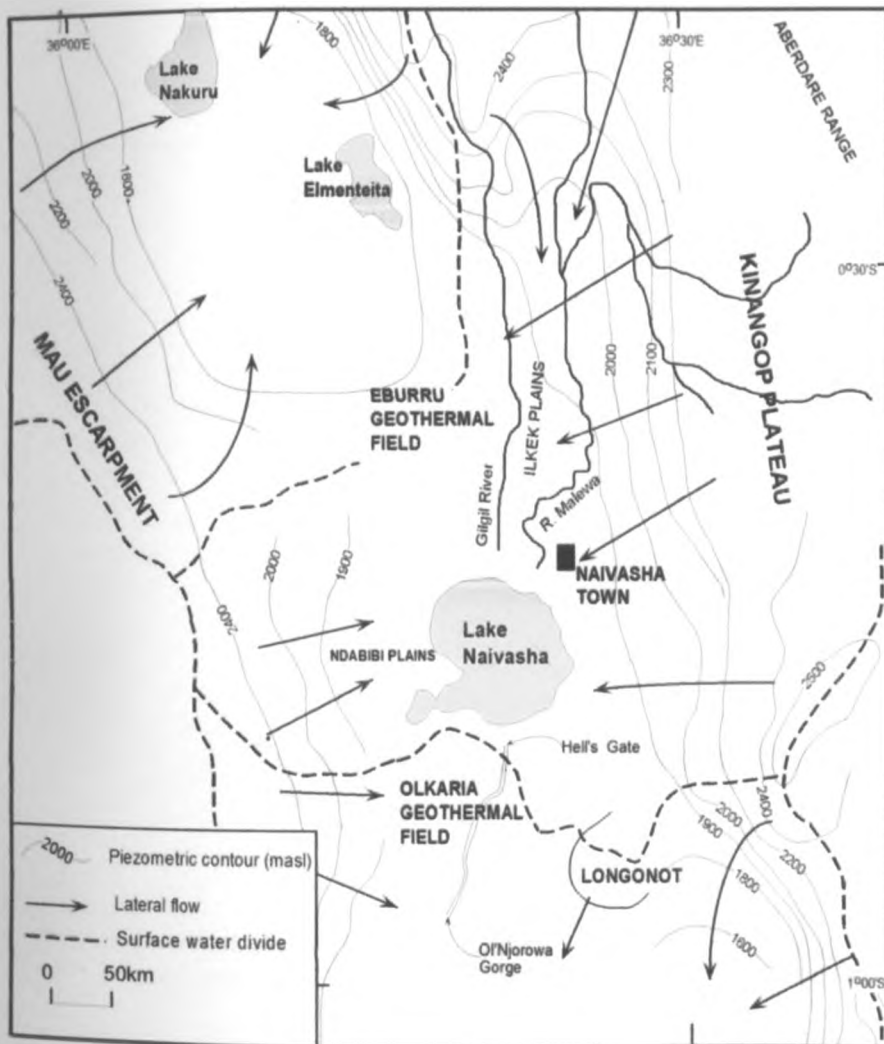


Figure 2.6: Regional hydrogeological map

The main recharge paths are the NNW-SSE and NW-SE east dipping Rift faults exposed on the Mau Escarpment. Rejuvenated N-S Rift floor faults and fractures control a lateral component of ground water flow into the geothermal system but have a shallower influence than the major rift forming faults that provide deep recharge. The regional NE and NW faults such as Olkaria fracture and Suswa lineament that cut across the Rift from the margins also contribute to local recharge into the geothermal system. Lake Naivasha is the main surface water body and contributes to the recharge of the system through a subterranean outflow system.

CHAPTER THREE

3.0 METHODOLOGY

The methodology adopted in this study was dedicated towards achieving the set objectives of the project. The main study themes included; review of the surface geology, review of petrochemistry data, lithological studies based on well logs and petrographic analysis to identify secondary or alteration minerals. Clay analysis for clay identification was also done and finally available chemical data of thermal fluids was used to calculate and predict subsurface temperatures. The project was conceived and undertaken in five main stages, the arrangement of the primary stages and the activities are presented by the flow chart in figure 3.1 below.

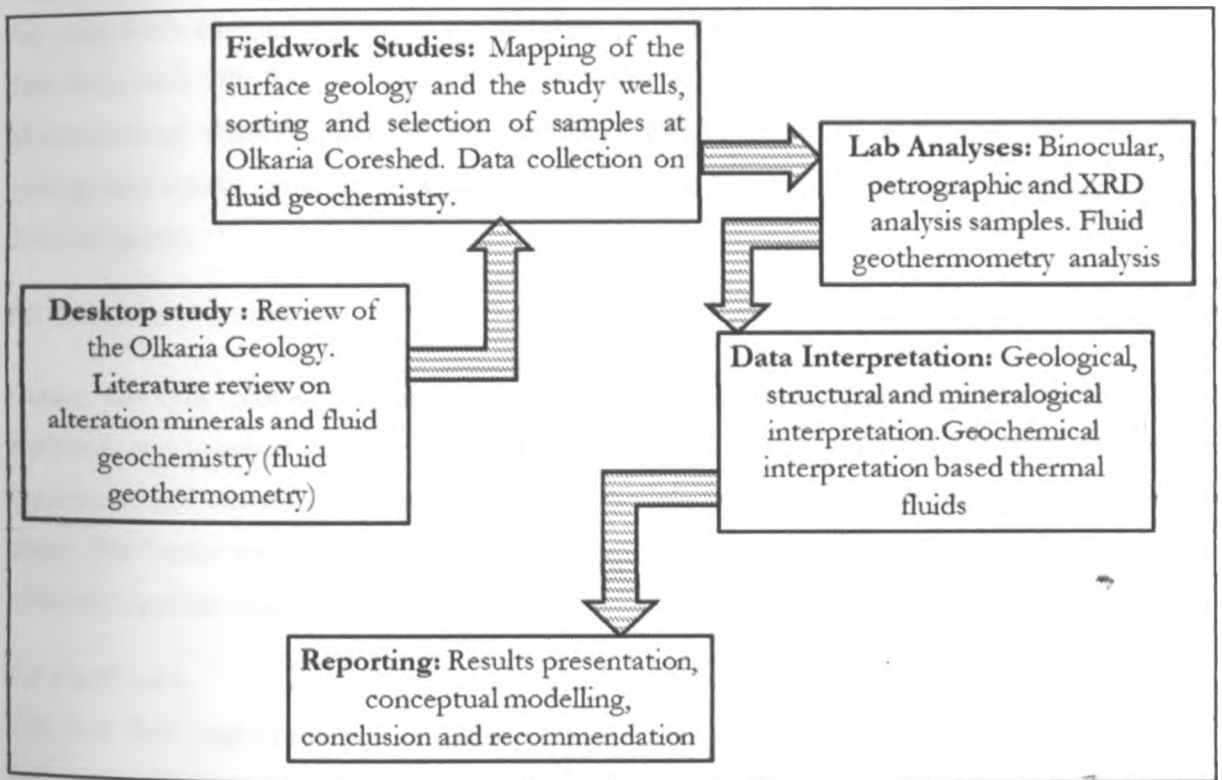


Figure 3.1: A flowchart of the five primary stages adopted in the study

The main materials used to accomplish the various tasks in this project included;

- Geological logs for wells OW-710, OW-23 obtained from Kengen.
- Geological map of scale 1:10000
- Topographical maps (Sheet No 133/4)
- Computer programs; ArcGIS, Rockworks and Canvas 9.

3.1 Data sourcing and handling

The data used in this report was made available by Kenya Electricity Generating Company and from laboratory analytic results. The data consisted of; the analyzed water samples, prepared geological logs and reports on the selected subfields. Major laboratory work was done on samples from well OW-912A since this was a new well while intermittent analysis was done on the other wells for quality control. For the purpose of this report, geological and geochemical data from wells OW-23, OW-710 and OW-912A were admitted. Out of the raw data from the aforementioned wells singling out the suitable analytical data that would best represent the geology and aquifer temperatures was done based on some important aspects e.g. representative data and quality.

3.2 Data interpretation

During this task geological maps were acquired and analytical data results obtained were analyzed and synthesized using various computer programs including; Surfer, ArcGIS, Rockworks and Canvas 9. ArcGIS and Canvas 9 were useful in digitization of georeferenced maps. The Surfer and Rockworks softwares were used to generate temperature Iso-maps and Litho-stratigraphic maps.

3.3 Field work

The first field exploration was undertaken from 2nd to 14th September 2010. The main work during this field work concentrated on well OW-912A, OW-23 and OW-710 and involved mapping of the wells (Figure 3.2). Selection of rock cuttings was done and specifically samples from OW-912A were sorted in the Coreshed. It is important to note the sampling guidelines as noted by Omenda (1998) were adhered to during sample selection and sorting such that samples.

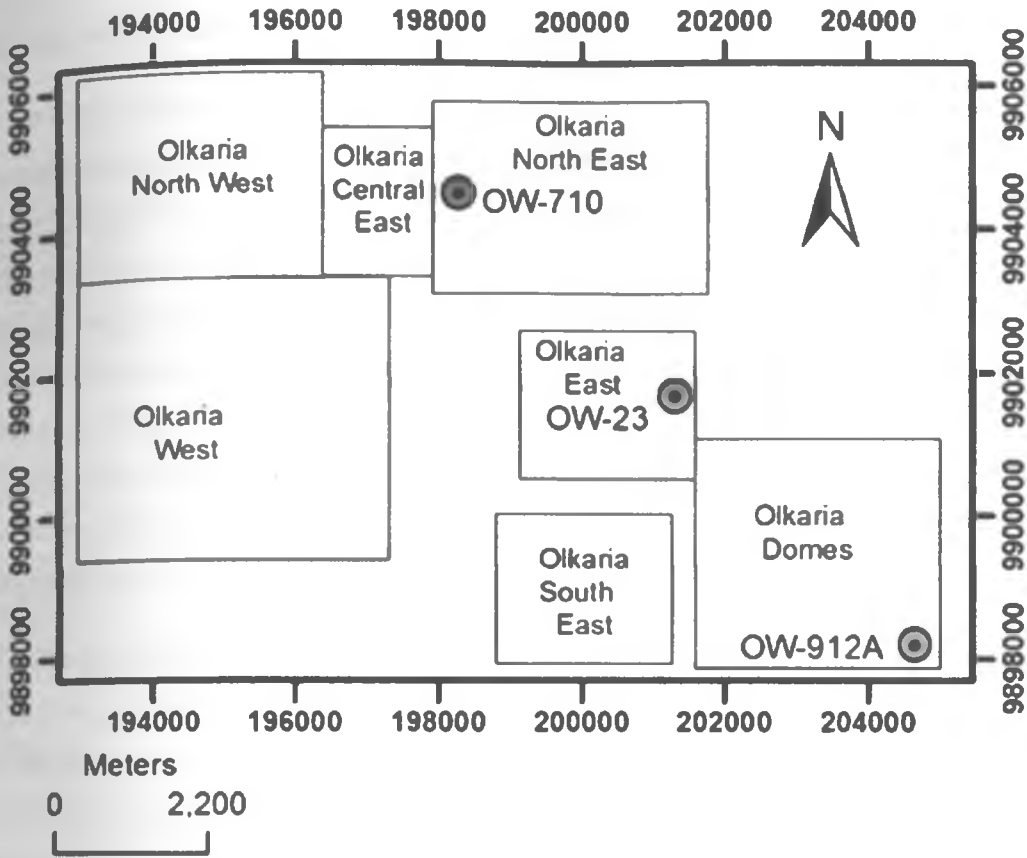


Figure 3.2: Location of study wells (modified from Muchemi 2000)

Preliminary analysis was done using a binocular microscope of the sample cuttings in order to identify lithological units penetrated, secondary minerals and subsurface structures. Sample cuttings were later selected at 50 meter intervals for XRD analysis. The second field campaign was undertaken from 2nd January to 12 January 2011. The work done during this period involved collection of data available on thermal fluid and subsequent analysis.

3.3 Laboratory methods

3.3.1 Stereo microscope analysis

Stereo microscope analysis is a visual method for preliminary analysis and semi quantitative form of describing rock and pore characteristics from drill cutting samples (Tiaine *et al.* 2002). The analysis during this stage was done using the Wild Heerbrugg binocular microscope. Each sample was scooped from the sample bag into a Petri dish and then washed with clean water to remove impurities and dust. Wetting the cuttings was necessary to enhance visibility of samples including obscure features such as finely disseminated sulphides e.g. pyrite. The sample was then placed on the mounting stage of the binocular microscope and among the essential features noted were the color(s) of the cuttings, rock types, grain size, rock fabric and original mineralogy, alteration mineralogy and alteration intensity.

3.3.2 X-ray diffractometer analysis (XRD)

The x-ray diffraction is used to identify individual minerals especially clays and zeolites (Cathelieu *et al.* 1985). The X-ray technique complements other methods, including optical light microscopy. Samples were selected from all the lithologic units in 50m interval and analyzed for clays. The <4 microns fractions were prepared for X-ray diffraction by use of a rock crusher. Finely grounded rock was then mixed with water to form a paste which was then mounted on a glass slide. A Shimadzu 600 diffractometer was used with $CuK\alpha$ radiation (at 40 kV and 50mA). Automatic divergence slit, fine receiving slit and graphite monochromatic count data were collected from 2° - 14° at intervals of 0.02° - 2θ for a period of 1 second. Count data were collected from 4° - 56° at intervals of 0.04° - 2θ for time of 1 second. The procedure of preparing clay sample preparations and XRD analysis are indicated in Appendix IA and Appendix IB respectively. The clay results for well OW-912A are tabulated in Appendix III.

3.3.3 Petrographic microscope analysis

Representative samples from all the lithological units encountered in well OW-912A were taken and thin sections were prepared for petrographic studies. The petrographic microscope was used to confirm the rock type, alteration minerals not observed by the binocular microscope and to study the mineralogical evolution.

CHAPTER FOUR

4.0 RESULTS

4.1 Surface geology of Olkaria

The surface geology of Olkaria area is very intricate and complex (Thompson and Dodson 1963). The main lithological units can be summarized as follows;

- Basalts
- Tephrites
- Trachytes
- Rhyolites
- Comendite
- Pyroclastics

Basalts

The Olkaria basalts are bluish grey and are younger compared to those that underlie Kinangop volcanics and the Kijabe basalts. They are vesicular with vesicles of up to 2.5 cm in diameter and may vary from finely porous rocks to scoracious. The basalts exposed at the periphery of the area are more porphyritic and slightly older than the others in area. The fine textured basalts that form cones near the southern end of the Ol'Njorowa Gorge are usually purplish maroon or reddish brown and finely textured rocks but porous. They are, however, extremely tough rocks containing few small plagioclase phenocrysts. The reddish color is due to erosion and oxidation hastened by the large surface area of those porous rocks. The coarse textured basalts are less prone to weathering and retain their typical bluish grey color.

Tephrites

A few small volcanic plugs project through the Gamblian lake beds west of Lake Naivasha and appears unrelated to the volcanism in the area. They are formed by rocks that are fine grained, bluish grey and sparsely distributed amygdaloidal vesicles. These rock are Tephrites and extend from west of Lake Naivasha to Ndabibi Plains.

Trachytes

Trachytes are found in most parts of Naivasha area occurring in both the Kinangop and Mau escarpments succession as valley lava flow and in the more Recent volcanic series of Longonot that extends to Olkaria. The trachytes are interbedded with the supposed Kamasian lacustrine deposited pyroclastics. They are grey medium to coarse grained porphyritic lavas. Weathering has altered their characteristic grey color to lighter shades of greenish gray. In more advanced stages of alteration, iron oxides are formed either in the phenocrysts or in a whole rock and appear as pale shades of maroon. Weathering frequently also accentuates fissility not apparent in fresh rocks and therefore trachytes frequently appear as fragments. The younger trachytes from Longonot volcano are fine grained and often highly vesicular making it easier to map their extents. Most of the agglomerates in the southern end of Ol'Njorowa Gorge are mainly trachytic in composition.

Rhyolites

Non comenditic rhyolite extrusions of the area are confined to an irregular area which curves around the south western shores of the lake. Other rhyolite craters and plugs are scattered along a line roughly parallel with the Ol'Njorowa Gorge. The rhyolites are younger than the comendites and may represent a later phase of volcanism involving common parent magma. In hand specimen they are pale grey, fined grained to porphyritic rocks with visible quartz. The pumiceous rhyolites are spongy like, highly porous and whitish to dirty grey and can float on water for a limited time.

Comendites

Sodic rhyolites of the Naivasha area have been variously described as comendite, pantellerite, quartz soda trachyte or simply soda rhyolite. The terms comendite and pantellerite are derived from the names of such localities as, comende in San Pietro Island south of Sicily and, the island of Panthellaria. In hand specimen they are dark colored with phenocrysts of quartz, alkali feldspars, aegirite, arfvedsonite or riebeckite or less common biotite. The comendites are fairly evenly distributed in the central portion of area. The most important exposures are the imposing

lava flows at the north entrance of Ol 'Njorowa Gorge and the columnar jointing flows which are about 107 m thick and form steep cliffs. Scenically the most impressive features are two comendite lava plugs known as Fischer's tower and horse (El barta) (Thomson and Dodson 1963).

Pyroclastics

Ashs, agglomerates and tuffs make up a considerable proportion of the volcanics in Olkaria field. Most volcanics or vents that have ejected ashes have the heaviest accumulations on the western sides of the cones due to a westerly prevailing wind during the eruption. The ashes are usually interbedded with other volcanics and have masked lava flows and structures in the area. Figure 4.1 give a geological map of the area showing the spatial relationship of the aforementioned lithologic units.

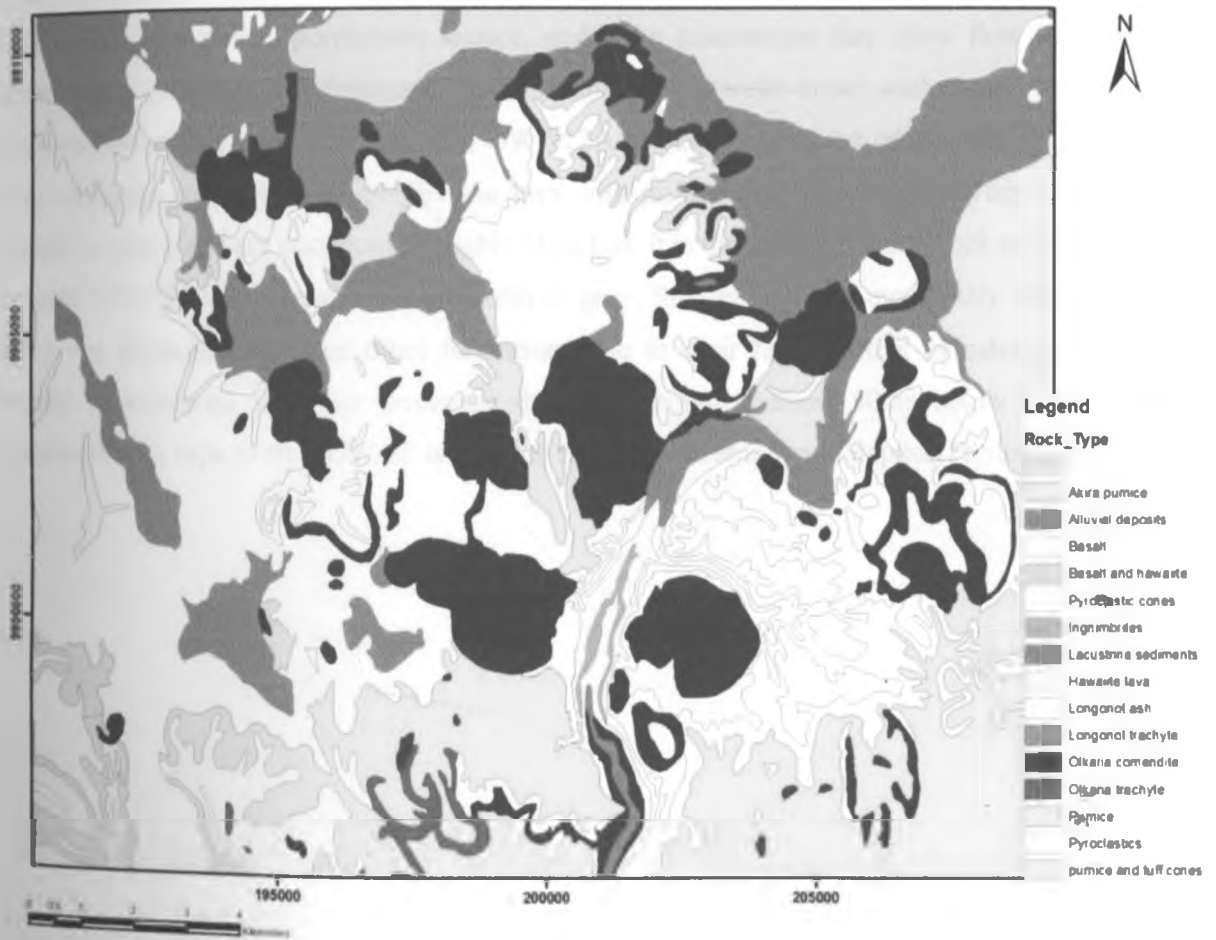


Figure 4.1: The geological map of Olkaria area (After Thompson and Dodson 1963)

4.2 Lithology

Wells OW-912A, OW-23 and OW-710 were drilled to depths of 3000 m, 1292 m and 1801 m respectively. The results from binocular and petrographic analysis show that the dominant rock unit is the pyroclastic and overlies basalts, trachytes, rhyolites and tuffs. The pyroclastics are yellowish brown and mainly made up of: pumice, obsidian and lava lithic fragments. They are encountered from the surface to about 50m below the surface. The tuffs, on the other hand, are brownish to reddish fine grained rocks. They are light in weight and moderately altered to clays. They are dominating in well OW-710 with a thickness of about 100m in sections where they are encountered (Figure 4.2).

The lava flows encountered are mainly rhyolitic, trachytic and basaltic. Rhyolites are light grey to grey in color with a porphyritic texture, under the microscope they show flow texture and phenocrysts of quartz and feldspars. They dominate in all wells under study, however they are encountered at shallower levels in well OW-912A as compared to the other wells (Figure 4.3). The trachytes are light grey, porphyritic lava with phenocrysts of feldspars. They are mainly altered to clays and are occasionally highly bleached. It is the most dominant rock unit especially in well OW-912A. The basalts are brownish to grey, fine grained and moderately altered lavas. They are distinguished from other formations due to their high content of calcite. They are mostly encountered at deeper levels the shallowest being at about 500m below surface. The dominant rock type in well OW-23 is trachyte encountered at extreme depths (Figure 4.4).

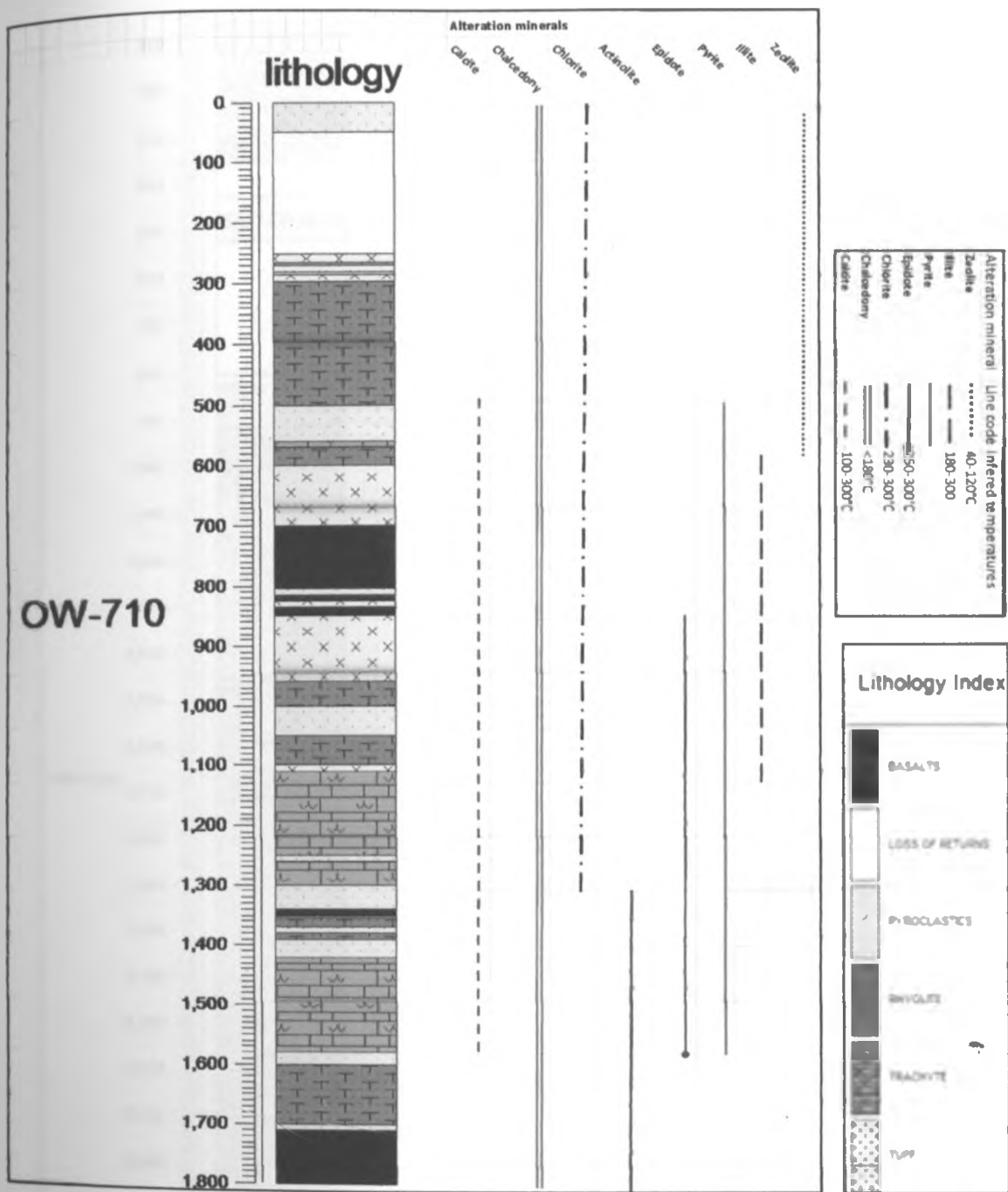


Figure 4.2: Lithology, distribution of hydrothermal alteration minerals and zonation in well OW-710 (Olkaria Northeast, depth is in meters)

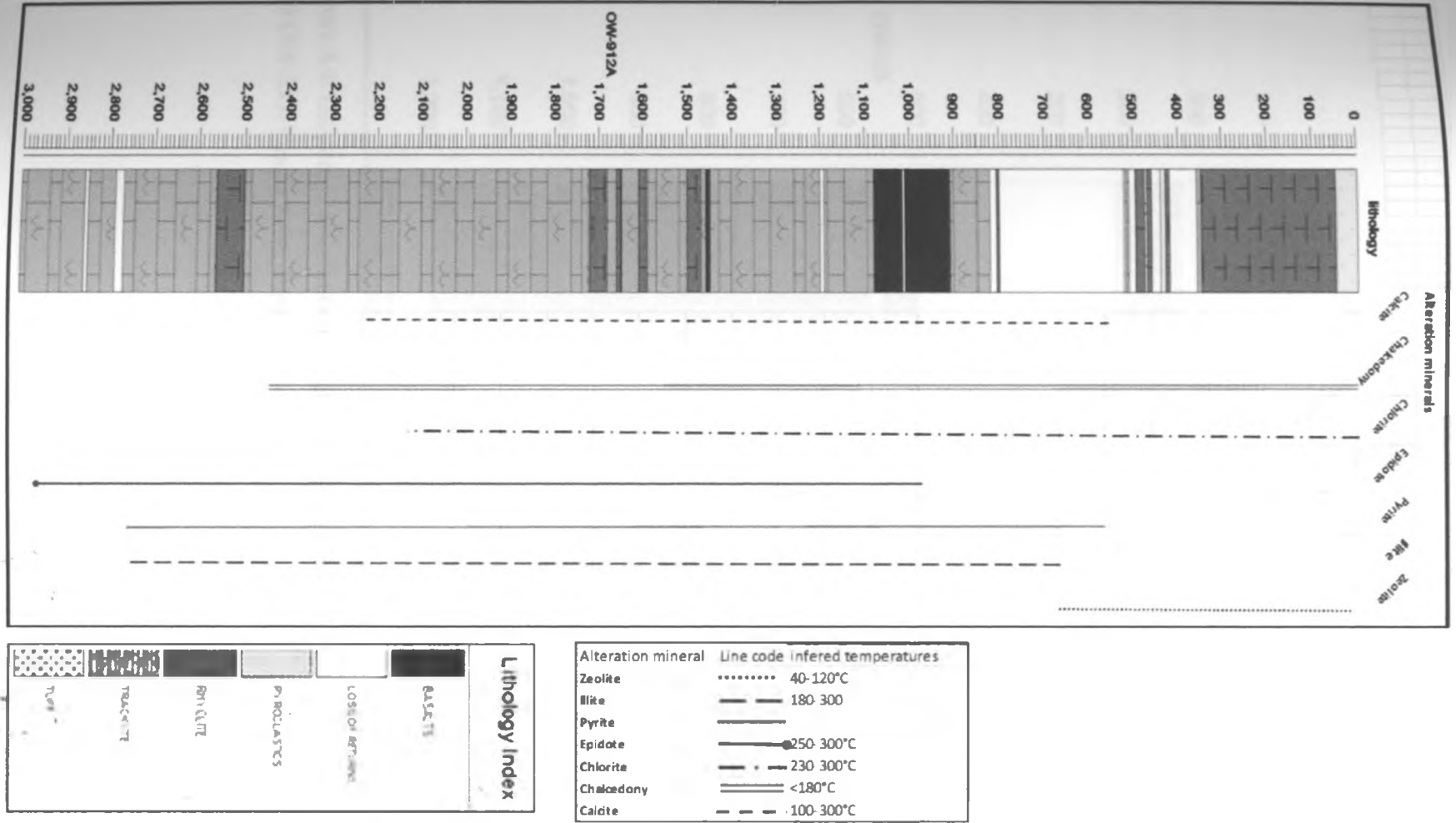


Figure 4.3: Lithology, distribution of hydrothermal alteration minerals and zonation in well OW-912A (Olkaria Domes, depth is in meters)

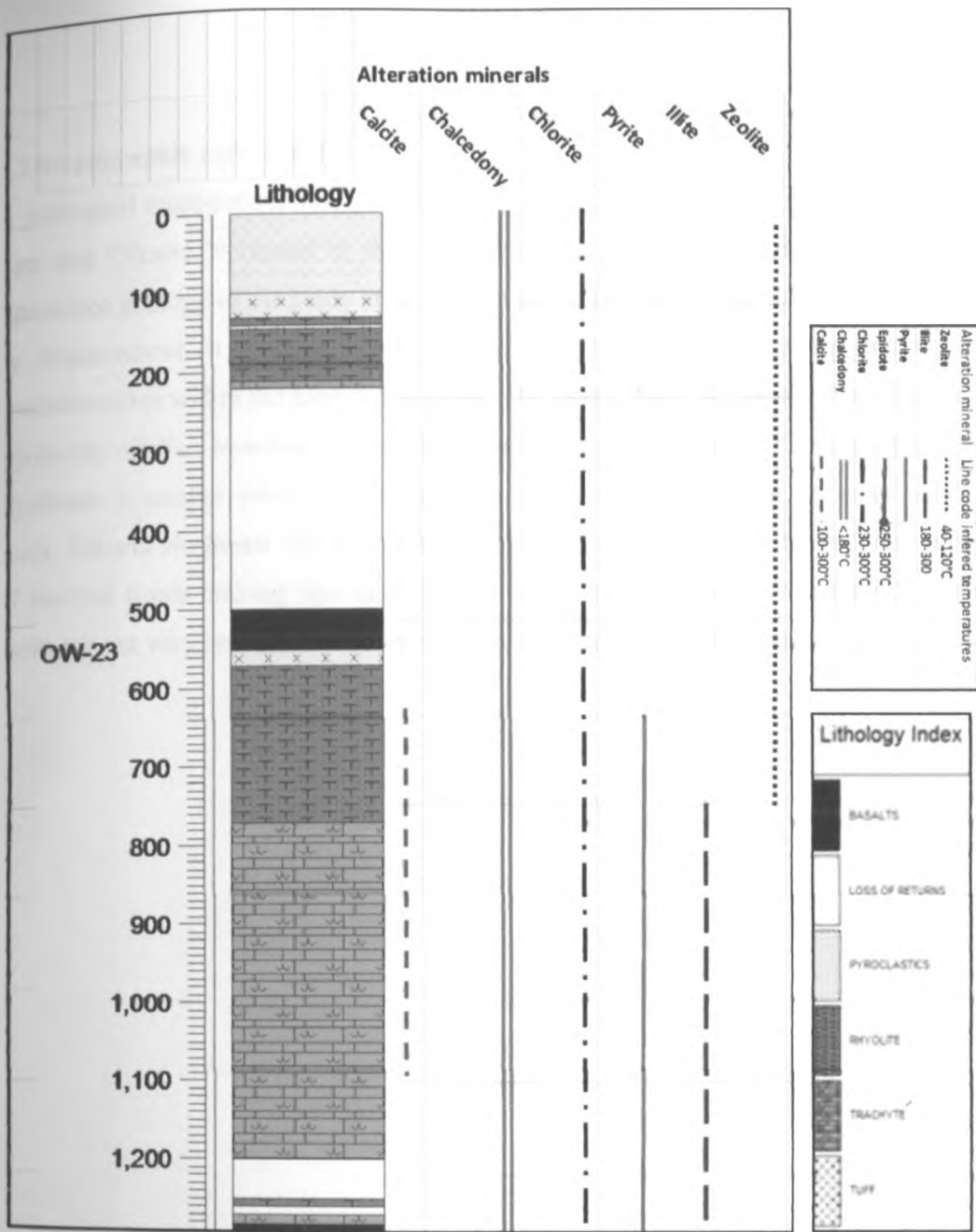


Figure 4.4: Lithology, distribution of hydrothermal alteration minerals and zonation in well OW-23 (Olkaria East, depth is in meters)

4.3 Stratigraphic correlation

A geological cross-section across wells OW-912A, OW-23, OW-710 in Olkaria Domes, Olkaria East and Olkaria Northeast is shown in Figure 4.5 below. The figure reveals in detail the subsurface geology of the study area. The structures in the area are faults and fractures indicated by displacement in the rock units and by loss of circulation during drilling resulting in unconformities within the lithological units. The stratigraphy of Olkaria Domes and Olkaria East are mostly similar, however, Olkaria Northeast is slightly different. The trachytic unit in Olkaria Northeast is smaller while the basaltic unit is thicker compared to the other subfields in this study. Olkaria Northeast and areas closer to Olkaria East are highly faulted, this favors the flow of thermal fluids making this subfield the most probable productive subfield, however, these faults are not very obvious on the surface due to thick pyroclastic cover.

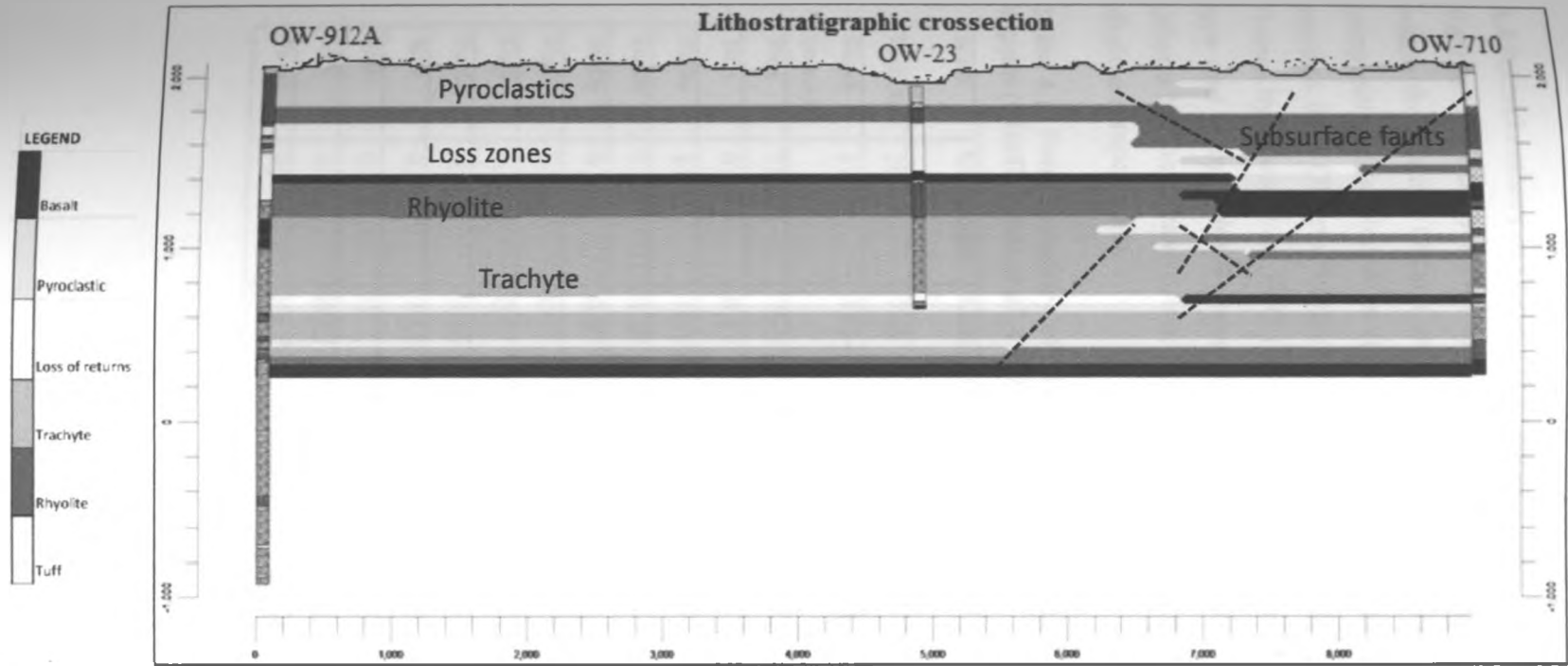


Figure 4.5: Geological cross-section between well OW-912A,OW-23 and OW-710

4.4 Petrochemistry of Olkaria field rocks

Various chemical analyses of surface and subsurface rock samples from the Rift flanks and within the Greater Olkaria show that, the volcanic complex is composed of rocks ranging in composition from basalt to rhyolite (Browne 1978, Omenda 2000). The chemical analyses of samples from Olkaria Northeast and Olkaria East fields by MacDonald *et al.* 1987 and Olkaria Domes by Black *et al.* 1997 (Tables 4.1 and 4.2) were important in determining the exact rock type and compositional variation. The results indicate that the rocks from Olkaria East and Olkaria Northeast have composition similar to those of Olkaria Domes generally with somewhat alkaline compositions.

Table 4.1: Petrochemistry of Olkaria Northeast and East fields. Oxides in % and elements in ppm (MacDonalds *et al.* 1987)

Rock	Comendite	Comendite	Trachyte	Rhyolite	Trachyte	Trachyte	Basalt	Trachyte
Wall No.	707	706	714	16	16	17	17	17
Depth (m.a.s.l)	1737	1834	1499	1193	751	1698	1386	702
SiO ₂	72.37	75.3	69.33	75.73	67.1	62.7	54.95	64.04
TiO ₂	0.34	0.17	0.48	0.33	0.72	0.62	0.42	0.8
Al ₂ O ₃	11.49	10.58	12.41	9.26	13.26	14.76	15.44	11.41
Fe ₂ O ₃	5.84	4.43	6.64	5.25	6.74	8	9.33	10.82
MnO	0.13	0.07	0.02	0.16	0.23	0.31	0.21	0.4
MgO	0.02	0	0.06	0.1	0.19	0.13	2.07	0.57
CaO	0.33	0.1	0.37	0.11	0.76	0.85	4.77	0.52
Na ₂ O	4.11	4.64	4.43	1.03	3.88	4.55	4.49	3.39
K ₂ O	4.9	4.53	4.94	5.64	5.45	5.65	3.05	3.76
P ₂ O ₅	0	0	0.02	0.02	0.07	0.06	0.34	0.09
LOI	0.4	0.22	0.55	1.86	1.01	2.13	3.37	3.14
Total	99.53	99.75	99.25	99.49	99.41	99.76	98.44	98.94

Table 4.2: Chemistry of Olkaria domes. Oxides %, elements in ppm (Black *et al.* 1997)

Rock	Rhyolite	Rhyolite	Trachyte	Basalt	Syenite
Well no	903	903	903	903	903
Depth M.L.s.l	1755-53	1537-35	1221-19	1141-39	209-207
SiO ₂	75.45	77.32	63.48	46.91	64.59
TiO ₂	0.14	0.13	0.46	2.11	0.81
Al ₂ O ₃	10.61	10.75	14.08	15.01	14.02
Fe ₂ O ₃	4.47	2.9	6.43	12.3	7.01
MnO	0.06	0.04	0.19	0.2	0.24
MgO	0	0	0.63	6.28	0.47
CaO	0.08	0.14	3.16	10.7	1.57
Na ₂ O	4.36	3.18	3.81	2.24	4.65
K ₂ O	4.44	5.220.01	5.53	0.84	4.96
P ₂ O ₅	0.01	0	0.05	0.21	0.1
LOI	0.33	0.29	2.15	3.02	0.87
Total	99.96	99.99	99.96	99.82	99.29

The Total Alkalis versus Silica (TAS) diagram in Figure 4.6 is developed from chemical analysis of the rocks from Olkaria East, Olkaria Northeast and Olkaria Domes fields. The plot shows that the samples mainly fall in the basaltic, trachytic and rhyolite portions in the TAS classification. This further helps in determining the exact rock types in the area.

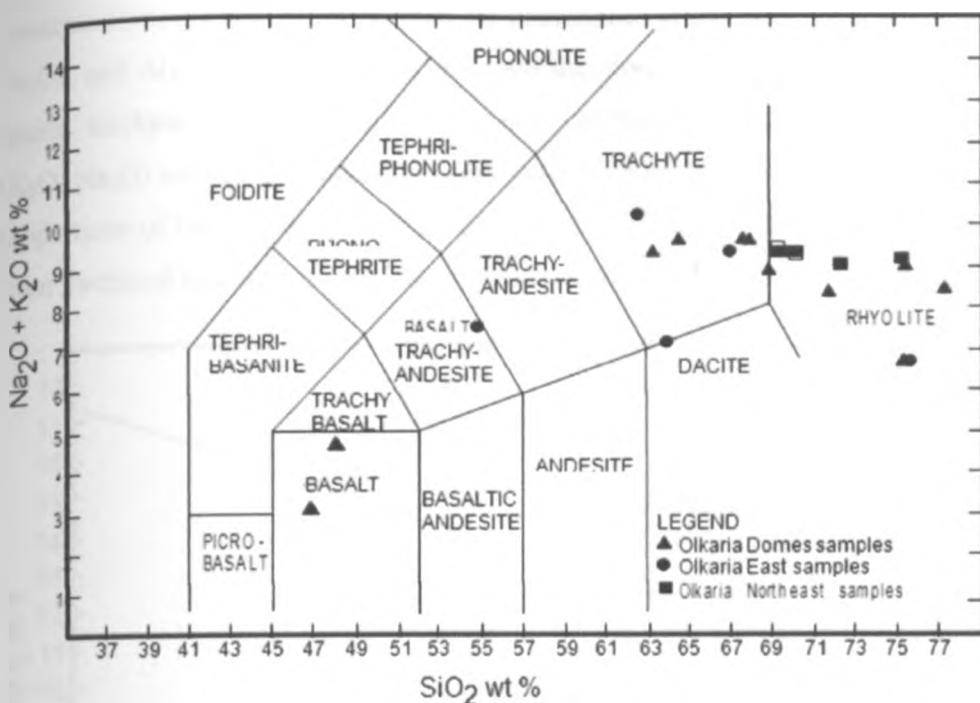


Figure 4.6: TAS Classification based on the petrochemical results of Table 4.1 and 4.2

According to Omenda (2000), the Olkaria comendites have high SiO₂ (71.8-77.3%) and are strongly depleted in TiO₂ (0.13-0.42%), MgO (0-0.16%), CaO (0.08-0.41%), and P₂O₅ (0.01-0.02%). Major element variation plots for trachytes and comendites show linear trends for the variation of TiO₂ and Fe₂O₃ (T) with SiO₂. The oxides Al₂O₃, CaO, Na₂O, and K₂O show the comendites fall on a trend that is at an angle to the trachyte trend. These trends suggest that most of the comendites are not related to the trachytes and to one another by simple fractional crystallization processes. However, those that lie on the same trend as the quartz trachyte genetically related.

Based on classification in terms of Al₂O₃-total iron as FeO diagram (MacDonald 1974) the Olkaria lavas are pantelleritic (Figure 4.7) and also fall in the comendite field. This classification separates comendites from pantellerite which have lower Al₂O₃, Fe₂O₃ (t), CaO, and Na₂O. Some of the samples plotting in the pantelleritic field have petrographic characteristics consistent with them being trachytes. These features include flow-aligned crystallites (Trachytic texture) and the absence of quartz phenocrysts. Their major element

concentrations are also different from the comendites in that they have higher contents of MgO, Fe₂O₃, and Al₂O₃ (12.5%). These rocks are therefore, true trachytes and can be referred to as quartz trachytes due to their high silica contents. The trachytes are typically potassic (K₂O > Na₂O) but the total alkalis are similar to those of the comendites, which have nearly equal proportions of Na₂O and K₂O. This classification indicates that pantellerite may have been formed from fractional crystallization of the comendites hence single source or same magma chamber.

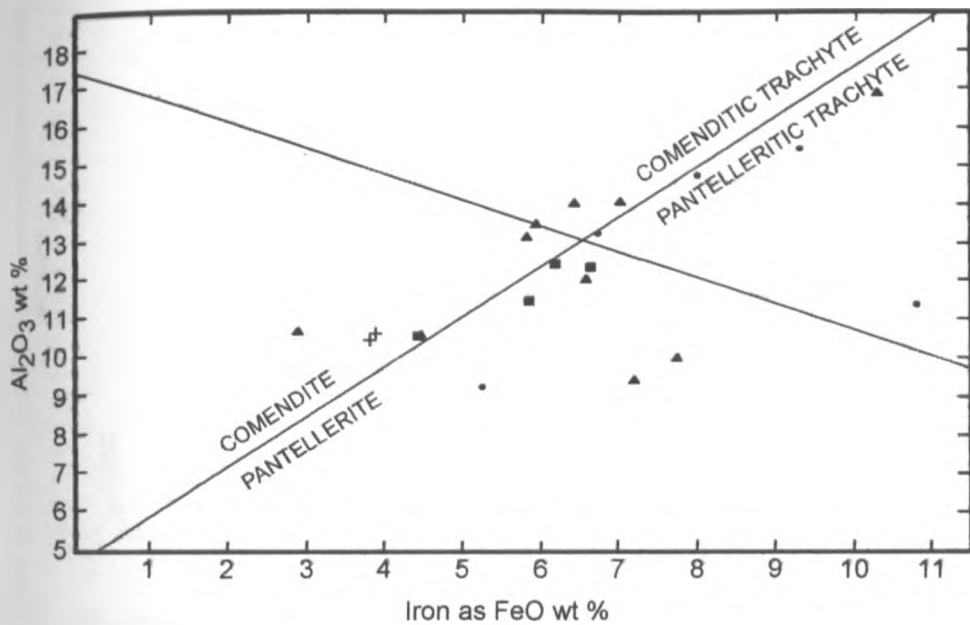


Figure 4.7: Classification in terms of Al₂O₃-total iron as FeO diagram (MacDonald 1974)

4.5 Description and distribution of hydrothermal alteration minerals

The distribution of hydrothermal minerals in wells OW-710, OW-912A and OW-23 is shown in the aforementioned Figures 4.2, 4.3 and 4.4 respectively. Below is a description of the hydrothermal alteration minerals encountered in the Olkaria Northeast, Olkaria Domes and Olkaria East wells.

Calcite

Calcite is a widely distributed alteration mineral occurring in all the three Olkaria wells. They are mainly deposited in Vesicles, fractures and as veins as white massive or colourless deposits. Calcite replaces plagioclase phenocrysts, pyroxenes and volcanic glass. The crystal

morphology of calcite is variable and ranges from individual thin-bladed crystals to equant needle-like crystals. Calcite crystals are deposited in veins at between 500 - 1600 m in well OW-710 (Figure 4.2) and 600-1100 m in well OW-23 (Figure 4.5). In well OW-912A calcite persist up to 2200 m (Figure 4.3). The calcite crystals were analyzed qualitatively by X-ray diffraction and the most intense peak ranged from about 3.02 to 3.05Å. A calcite diffractogram is shown in Figure 4.8.

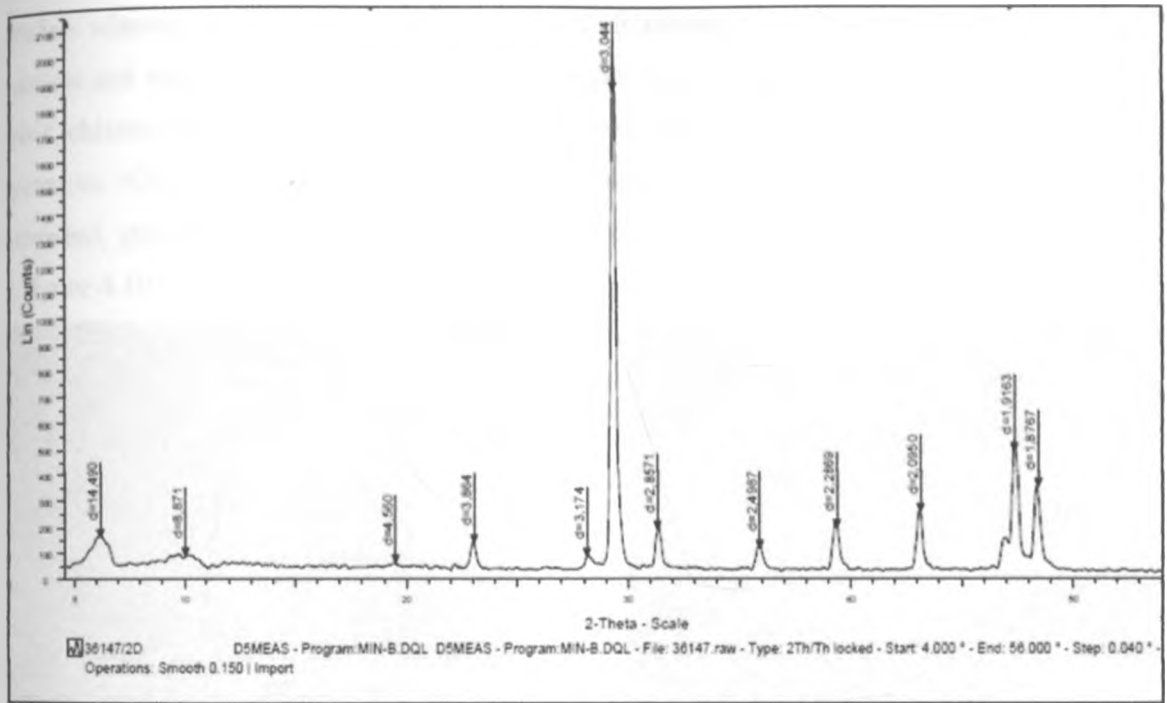


Figure 4.8: Diffractogram of calcite showing a strong peak at 3.044Å

Chalcedony

Chalcedony occurs from the surface to the bottom in all the study wells except in well OW-912A where it disappears at 2500 m. They are cryptocrystalline and range from colourless, white, or bluish-grey in colour. They are deposited in vesicles, fracture and also as veins. They generally have massive, banded or botryoidal texture. At greater depths where temperatures are high, chalcedony in vesicles is transformed or was completely transformed into quartz but the chalcedonic texture was still preserved.

Chlorite

Chlorite occurs between 0 and 1300 m in well OW-710, 0 and 1250 m in well OW-23 and 438 to 1940 m in well OW-912A (Appendix III). Chlorite shows a wide distribution and a big variability in colours, forms and textures. It varies in colour from light-to-dark green, has low birefringence and occasionally shows anomalously blue, brown or purple interference (Figure 4.9). In the upper levels of the volcanic sequences, chlorite appears in small intergranular patches whereas at the deepest levels, chlorite is idiomorphic and forms in radial aggregates in veinlets and vugs in association with: quartz, calcite, epidote, amphibole and pyrite. Within the veins, chlorite occurs as microspherules enclosed within epidote, but it may also replace primary pyroxene. XRD analyses of chlorite show conspicuous peaks at 7.0-7.2Å and 14.0-14.5Å in the untreated, glycolated and oven heated samples. A diffractogram indicative of chlorite is shown in figure 4.10.

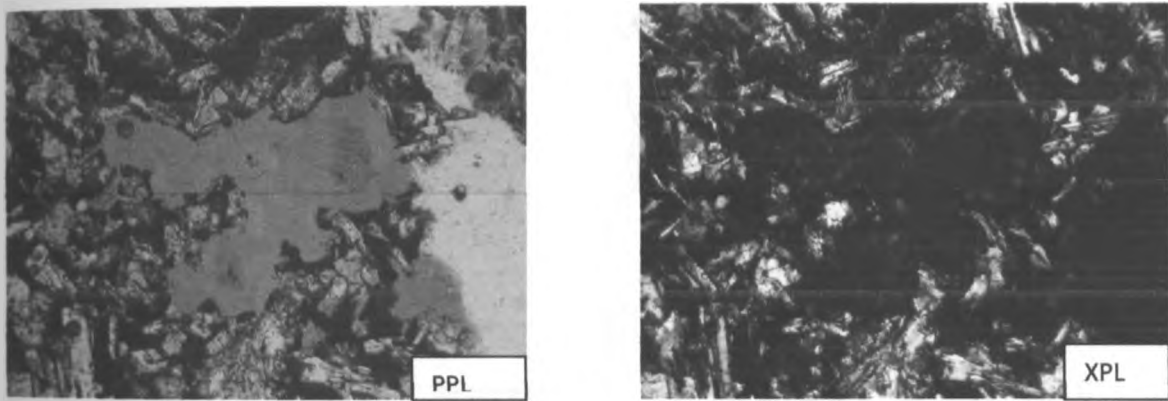


Figure 4.9: Vesicle filling chlorite In thin section showing a low birefringence and an anomalously blue, brown and purple interference

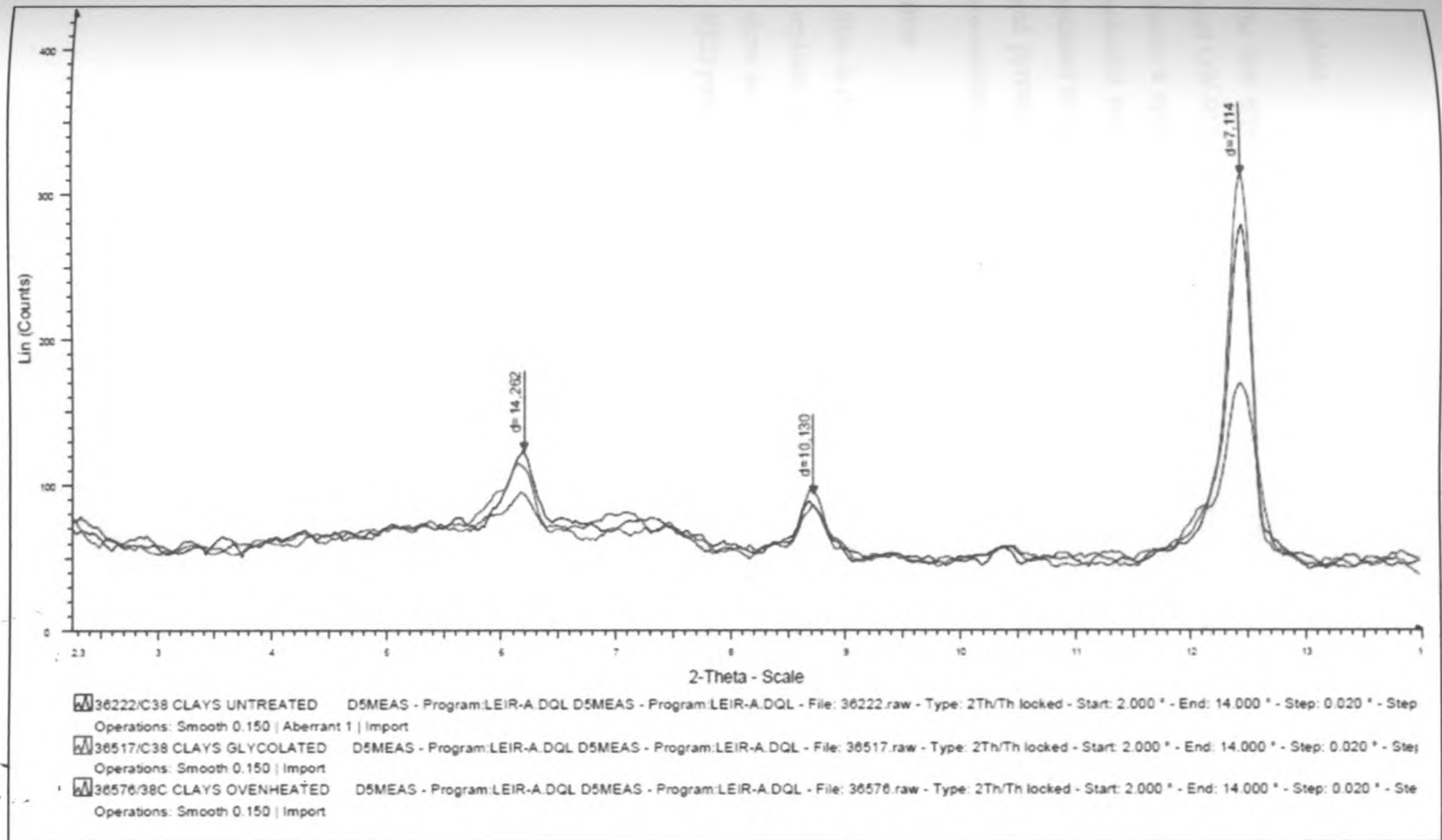


Figure 4.10: Diffractograms of clays showing unchanged peaks at 7.11Å and 14.2 Å for chlorite and 10.13Å for illite in the Air dried, glycolated and the oven heated samples

Epidote

The first appearance of epidote is from 850 m and is evident up to 1580 m in well OW-710. In well OW-912A it occurs between 1000 and 2900 m, however it is absent in well OW-23. Epidote shows a systematic textural development with increasing depth. In shallow zones crystals are anhedral and form fine grained aggregates and in deeper zones they are idiomorphic, tabular, radiated or fibrous. Epidote is found filling fractures, vesicles, and replacing primary plagioclase and pyroxene and in most cases forms mineral associations with mainly quartz, chlorite and sometimes calcite, wairakite and pyrite.

Illite

Illite is detected below 600 m in the three wells. The mineral is light green to white in colour, replaces K-feldspar and occurs as a vein and vesicle filling mineral. XRD analyses of illite show no change at the 10 Å in the untreated, glycolated and oven heated samples. An illite XRD pattern clearly indicating the 14 Å and 10 Å d-spacing is shown in figure 4.11.

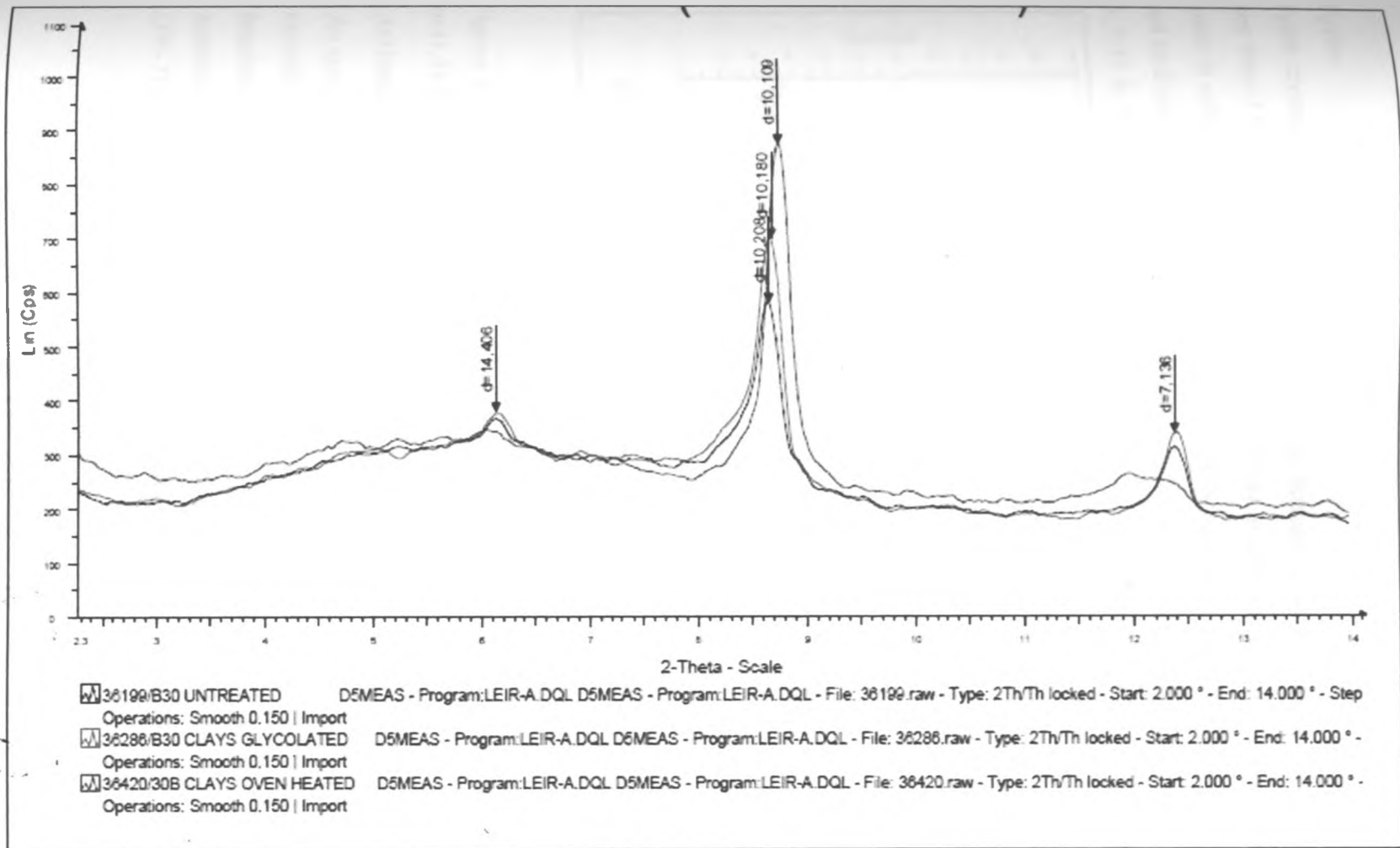


Figure 4.11: Diffractograms of clays showing strong illite peaks at around 10\AA and minor chlorite component with peaks at 7.14\AA and at 14.41\AA in the Air dried, glycolated and the oven heated samples

Pyrite

Pyrite crystals are present below 500 m to the bottom in the three wells, however, they become rare from 1580m in well OW-710. Pyrite occurs as euhedral cubic crystals with brassy yellow luster in reflected light. Tiny cubic pyrite crystals were deposited in fractures, vesicles and veins and as disseminations in the groundmass. XRD analysis of pyrite indicates strong peaks at 3.13 Å, 2.71 Å, 2.42 Å, 2.21 Å and 1.91 Å as shown in the XRD diffractogram (Figure 4.12).

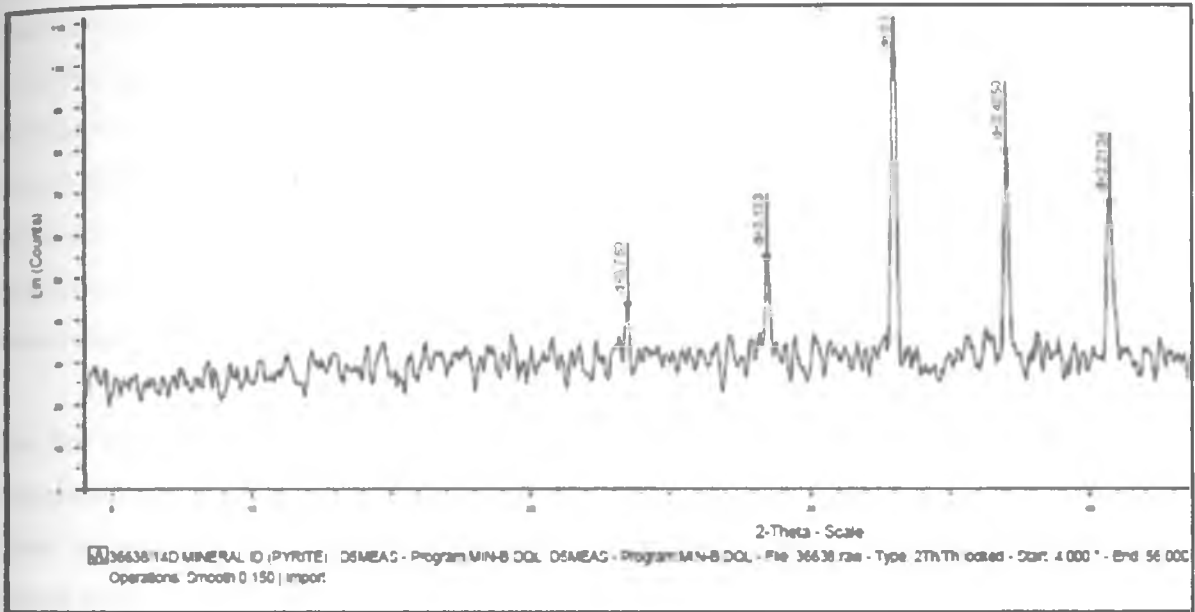


Figure 4.12: Diffractogram of pyrite showing strong peaks at 3.13Å, 2.71Å, 2.42Å, 2.21Å and 1.91Å

Actinolite

An actinolite mineral is green to greyish green in colour, and forms radiating fibers or acicular crystals and also massive to granular aggregates in the groundmass and has a moderate birefringence. The mineral is formed as a replacement of ferromagnesian minerals in association with epidote and chlorite. Actinolite appeared in the deeper hotter parts of well OW-710 but was conspicuously absent in well OW-912A and OW-23.

4.6 Hydrothermal zonation

Based on this study encountered mineral assemblages in Olkaria have been grouped into four basic depth and temperature related alteration zones. The zeolite-chlorite-(smectite) zone (1), initiated around 40°C, reflects the alteration of the most unstable primary minerals, namely volcanic glass and olivine, into smectite clays (Fe-rich saponites) and a variety of low-temperature Ca-Si zeolites including analcime, clinoptilolites and stilbite. There is a transition zone of mixed-layer clay defined by the point at which smectite starts to become unstable (~200°C) and is gradually replaced by an inter-stratified smectite-chlorite. The underlying illite-chlorite zone (2) is characterized by the presence of discrete chlorite, which begins to form around 230°C (Lagat 2004). The chlorite-epidote-illite zone (3) correlates with the first appearance of epidote, believed to form at temperatures exceeding 230-250°C. Other temperature dependent minerals associated with the latter two zones include the high-temperature zeolite wairakite (>200°C), prehnite (>240°C) and wollastonite (>260°C).

The first appearance of the amphiboles and actinolites formed by the alteration of pyroxene at temperatures exceeding 280°C, defines the epidote-actinolite zone (4). At Olkaria, grossular garnet has also been sporadically identified within these zones (Browne 1981) and at the deepest, hottest parts (>350°C). In addition to the minerals described above, pyrite is widespread across the entire temperature range and its abundance is believed to be controlled by the system permeability and supply of H₂S (e.g. Reyes 1990). Calcite is also abundant in well-cuttings, with its stability extending to temperatures around 290-300°C. Chalcedony and amorphous silica are observed at temperatures below 180°C, but at higher temperatures crystalline quartz is formed. Other secondary minerals that are typically identified in Olkaria geothermal system include: pyrrhotite, chalcopyrite, sphalerite, apatite and titanite.

Lagat (2004) described the depth-zonal distribution of some of the main temperature dependent alteration minerals throughout the domes subfield – quartz (>180°C), epidote (>230-250°C), wollastonite (>260°C), and Al-free amphibole (>280°C). A cross-section through Olkaria Domes, Olkaria East and Olkaria Northeast subfields showing the hydrothermal zonation is shown in figure 4.13. The cross-section shows the four zones describe above.

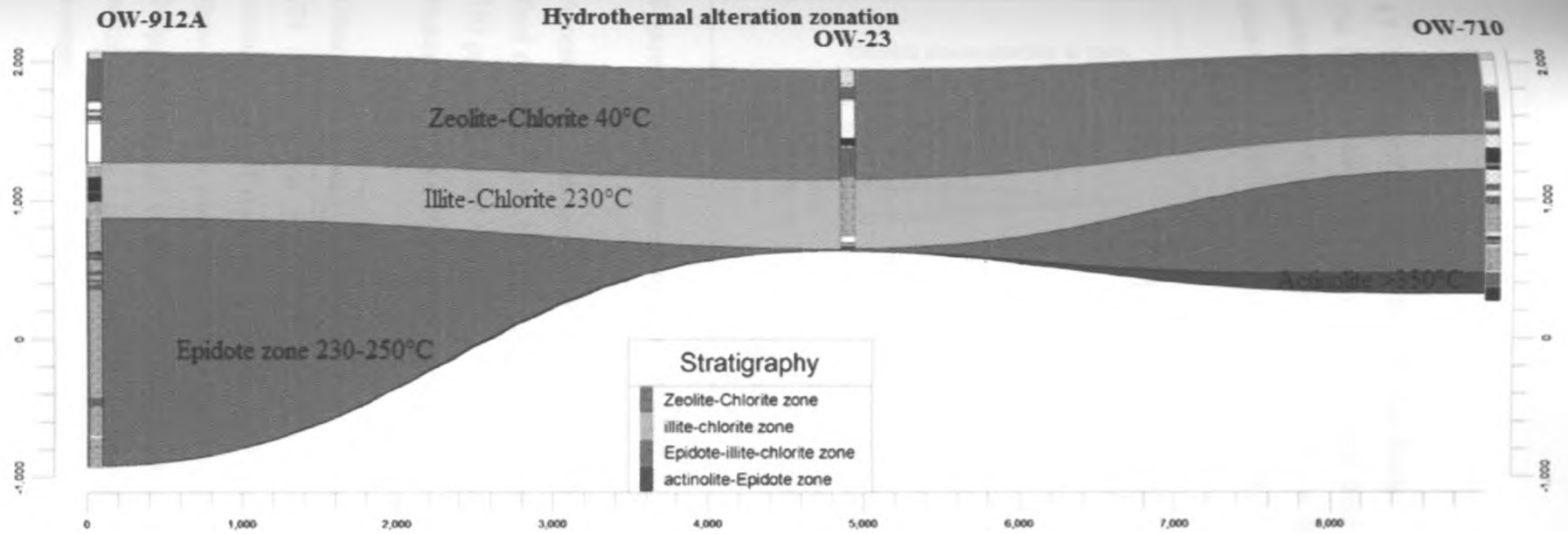


Figure 4.13: Distribution of hydrothermal mineral zonation with depth across wells OW-912A, OW-23 and OW-710 in Olkaria geothermal field (Units in meters)

4.7 Fluid geochemistry of the Olkaria fields

The fluid chemistry of Olkaria geothermal field has marked similarities and variations from subfield to subfield and sometimes from one well to another. Chloride concentration variations from various subfields are indicated in figure 4.14 below.

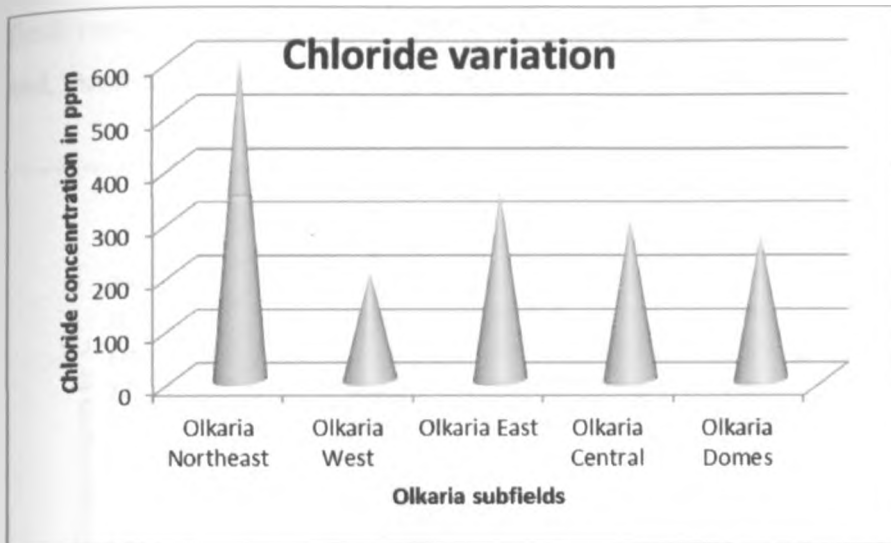


Figure 4.14: Average chloride concentration from Olkaria fields

According to Karingithi (1992, 1993, 1996), Karingithi and Wambugu (1997) the Olkaria East fluid discharges rich bicarbonates-carbonate concentration of 200ppm and Cl^- concentrations of 350 ppm. While the Olkaria North east fluids are bicarbonate-carbonate waters with relatively higher Cl^- concentrations of 600 ppm.

Olkaria central wells results indicate Cl^- concentrations of about 300ppm except for well OW - 201 which gives high values of 700 ppm. Olkaria central wells have relatively high concentrations of reservoir CO_2 concentrations, therefore they are bicarbonate waters similar to those in Olkaria west field (Wambugu 1995), and have high chloride concentration of about 200ppm compared to those from Olkaria East. Karingithi (1999) suggested that Olkaria domes wells discharge mixed sodium bicarbonates-chloride- sulphates fluids with chloride concentrations of 270 ppm.

4.8 Solute geothermometry

The temperature functions of Fournier and Porter (1982) for quartz geothermometers, Fournier (1979) and Giggenbach (1988) for Na/K are utilized in the estimation of the reservoir temperatures. Reservoir temperatures calculated based on the K/Na ratio indicates aquifer temperature values at Olkaria East fields as 250°C (Arnorsson *et al.* 1983). Olkaria Northeast fields results indicates values of 290°C on average (Figure 4.15), however K/Na data is limited and, therefore, in the current study quartz geothermometry is applied.

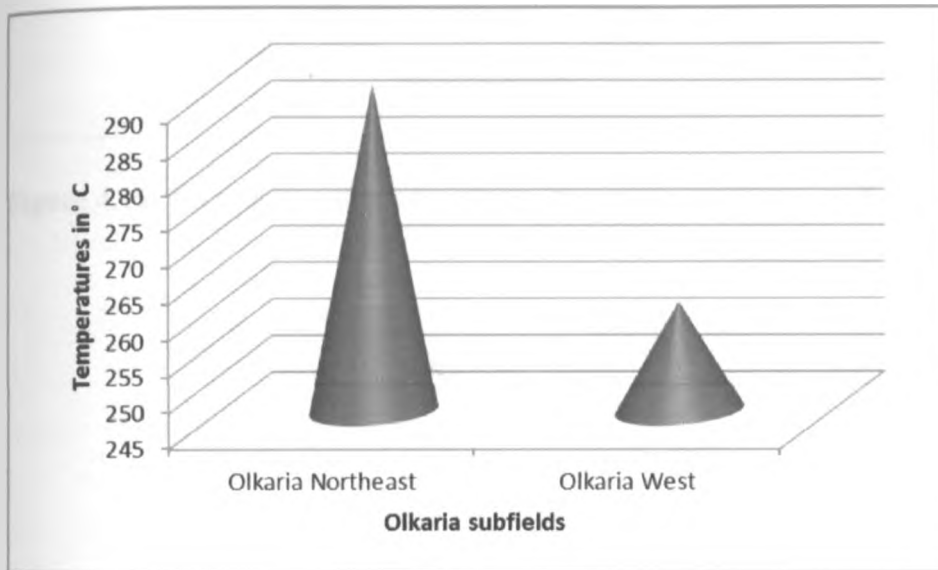


Figure 4.15: Temperatures inferred from the K/Na ratios

According to Fournier and Potter (1982), quartz geothermometry indicates that Olkaria East wells have reservoir temperatures of 260°C. The Olkaria Northeast wells have values of 270°C while Olkaria central and Olkaria domes is 259°C about 236°C respectively (Figure 4.16). There is a significant reduction in temperatures towards Olkaria west field to values of about 180°C.

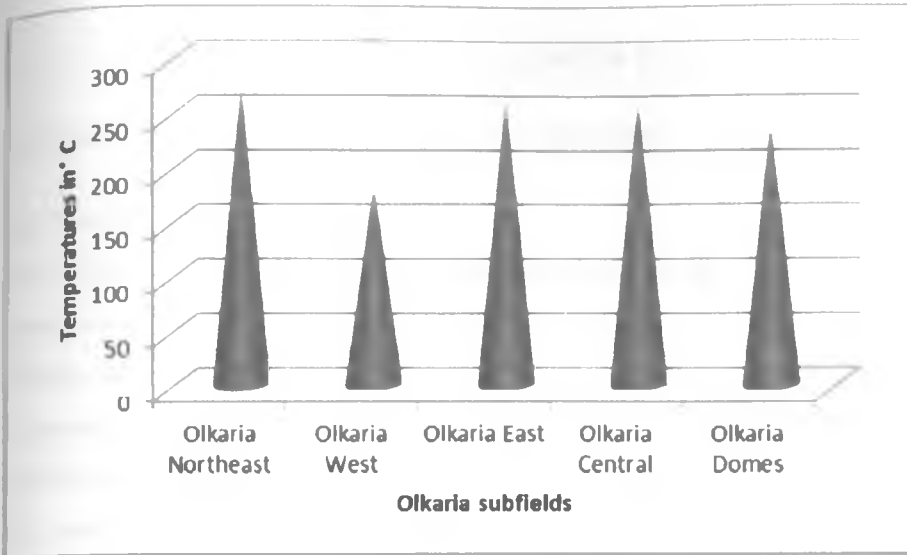


Figure 4.16: Temperatures inferred from the quartz geothermometry

CHAPTER FIVE

5.0 DATA SYNTHESIS AND THE CONCEPTUAL MODELING

5.1 Geology and petrochemistry

The Olkaria geothermal system is characterized by complex tectonic activity associated with the evolution of the Eastern African Rift System (EARS). The volcanism is thought to have started during the Pleistocene period and resulted in various geomorphologic features including the Longonot and Eburru volcanoes. The hydrogeology of Olkaria area is strongly controlled by the eastern and western rift flank faults, the rift floor faults and the rock types. The main recharge for the system is mainly from the rift faults and the NNW-SSE faults. The rock petrochemistry reveals that the rocks in the area are not related genetically by simple fractional crystallization.

5.1.1 Surface geology of Olkaria

The surface geology as revealed by field data can be divided into five main rock types namely; basalts, trachytes, rhyolites, comendite and pyroclastics. The Olkaria basalts are younger compared to those that underlie the Kinangop volcanics and the Kijabe basalts. They form cones near the southern end of the Ol'Njorowa Gorge and are usually reddish brown and finely textured but porous rocks. They are, however, extremely tough rocks containing small plagioclase phenocrysts. The trachytes are found in more recent volcanic series of Longonot and extend to Olkaria. The trachytes are interbedded with Kamasian lacustrine sediments and pyroclastics. Older trachyte frequently appears as fragments in younger agglomerates with some of these agglomerates being exposed at the southern end of Ol'Njorowa Gorge. The younger trachytes from Longonot volcano are fine grained and often highly vesicular with few exceptions being non-porphyrific.

Non-comenditic rhyolite extrusions of the area are confined to an irregular area which curves around the south western shores of the Lake Naivasha. Other rhyolite craters and plugs are scattered along a line roughly parallel to the Ol'Njorowa Gorge. The rhyolites are younger than the comendites and may represent a later phase of volcanism involving common parent magma. Sodic rhyolites of the Naivasha area have been described as comendites and are distributed fairly

even in the central portion of area (Omenda 2000). The most important exposure is the lava flows at the north entrance of Ol 'Njorowa Gorge and the columnar jointing flows. They are about 107 m thick and form steep cliffs often capped by a skin of black obsidian presumably of the same composition. Volcanic ash, agglomerates and tuffs make up a considerable proportion of the volcanics in the Olkaria area and most vents (Eruption centers) that ejected the ashes have the heaviest accumulations on the western sides of the cones due to an easterly prevailing wind during the eruption.

5.1.2 Lithostratigraphy

The lithostratigraphy of Olkaria geothermal field as revealed by well log data indicate that Olkaria Domes area is composed of pyroclastic, tuff, rhyolites, trachyte and basalt. The Olkaria Northeast comprises of tuff layers and basalts with intercalations of pyroclastics. However, the basalt layer is more pronounced in this field. In Olkaria East the trachyte and rhyolite are the major lithological units. Subsurface structures inferred from noticeable displacements in the rock units and by loss of circulation/returns in the reconstructed lithostratigraphy are faults and fractures around Olkaria Northeast and Olkaria east subfields. The structures are not seen on surface due to pyroclastic cover masking the area.

Permeable zones in the wells were interpreted by loss of circulation/returns and hydrothermal alteration mineralogy patterns. Loss of circulation/returns recorded at shallow depths above the groundwater table due to a fractured rhyolite lava. Well OW-912A generally has good permeability compared to the other wells under study, this is inferred from the lithostratigraphy indicating major loss of returns or circulation (Figure 4.3). In Well OW-710 loss of circulation/returns is experienced mainly at shallow depths while in Well OW-23 the losses were encountered at 500 m and at 1200 m.

5.1.3 Petrochemistry

The chemical analysis of the rocks from Olkaria East, Olkaria Northeast and Olkaria Domes fields indicate that rocks from Olkaria East and Olkaria Northeast have compositions, similar to those of the Olkaria Domes generally with somewhat alkaline compositions. The Olkaria comendites have high SiO_2 (71.8-77.3%) and are strongly depleted in TiO_2 (0.13-0.42%), MgO (0-0.16%), CaO (0.08-0.41%), and P_2O_5 (0.01-0.02%). The trachytes have relatively low values

of SiO₂ (62.7-69.3%) and slightly higher values of TiO₂ (0.72-0.8%), MgO (0.13-0.19%), CaO (0.52-0.85%), and P₂O₅ (3.76-5.65%). The basalts have low SiO₂ (54.95%) but are highly enriched in CaO (4.77%). Major element variation plots for quartz trachytes and comendites show linear trends for the variation of TiO₂ and Fe₂O₃ with SiO₂. The oxides Al₂O₃, CaO, Na₂O, and K₂O show that the comendites fall on a trend that is at an angle to the quartz trachyte trend. These trends suggest that most of the comendites are not related to the quartz trachytes and to one another by simple fractional crystallization processes.

Based on classification in terms of Al₂O₃ and total iron (FeO), the Olkaria trachytes are pantelleritic and have higher Al₂O₃, Fe₂O₃, CaO, and Na₂O. Their major element concentrations are also different from the comendites in that they have higher contents of MgO, Fe₂O₃, and Al₂O₃ (12.5%). However the petrographic characteristics are consistent with them being trachytes. These features include flow-aligned crystallites (Trachytic texture) and the absence of quartz phenocrysts. These rocks are, therefore, true trachytes and can be referred to as quartz trachytes due to their high silica contents.

5.2 Fluid geochemistry and geothermometry

Thermal fluids in Olkaria West field contrast sharply with those in the fields under study. In the Olkaria West field, the discharge fluids are typically rich in bicarbonates but the chloride content is very low. The Olkaria East fluid discharges have similar bicarbonates-carbonate concentration of <200 ppm as those in the Olkaria Northeast but low chloride concentrations of 200-350 ppm. Fluid geochemistry indicates high chloride concentration in the Olkaria Northeast field; this means the fluids are typically geothermal waters. Permeability is a factor here, the deep fractures and faults providing channels for chloride anions from a magmatic source to admix with thermal fluids and reach the surface. Olkaria Domes wells discharge is of a mixed sodium bicarbonate-chloride-sulphate type with low mean chloride concentrations of 181.5-269.9 ppm indicating bicarbonate and chloride thermal fluids are mixing.

Reservoir temperatures have been calculated using chemical geothermometers and the results indicate that the K/Na ratio function by Arnorsson *et al.* (1983) gives average reservoir temperature values of 258°C for the Olkaria West and 290°C for Olkaria Northeast (Figure 4.15).

Reservoir temperatures calculated using the quartz geothermometry function by Fournier and Potter (1982) show Olkaria East wells have reservoir temperatures of 255°C. The Olkaria Northeast wells have values of 270°C while Olkaria Domes field have values of 240°C (Figure-4.16).

5.3 Hydrothermal alteration and zonation

The upper 50 m of lithostratigraphy in each well is unaltered and is mainly composed of pyroclastics. The zone immediately below is zeolite-chlorite alteration which represents low grade alteration. Minerals characterizing this zone include zeolites, chlorite, chalcedony, pyrite and calcite. The illite-chlorite zone is not extensive as the zeolite-chlorite zone and occurs below 700 m deep in each well, the index minerals in this zone are illite, chlorites and pyrites. The moderately high temperature zone of chlorite-illite-epidote zone occurs below 1200 m and the main index mineral is epidote indicating temperatures of over 250°C. The hottest zone is the actinolite-epidote zone (Table 5.1) which is over 1500m deep in well OW-710. The mineral assemblages (Epidote and actinolite) representing this zone were not observed in well OW-912A and in OW-23 indicating that it is confined to well OW-710. Well OW-710 is therefore located above a hot area probably overlying a hot plutonic body.

Table 5.1: Hydrothermal alteration mineral in the study wells (X indicate presence of mineral)

Hydrothermal alteration minerals.	OW-710	OW-23	OW-912A	Temperatures
Zeolite	×	×	×	40-120°C
Pyrite	×	×	×	-
Calcite	×	×	×	100-300°C
Chalcedony	×	×	×	<180°C
Illite	×	×	×	180-300°C
Chlorite	×	×	×	230-300°C
Epidote	×		×	250-300°C
Actinolite	×			>300°C

5.4 Conceptual model

The development of a conceptualized model of the Greater Olkaria geothermal area was first proposed by Sweco and Virkir (1976) and since then a model has been developed in the Olkaria Domes area. The model developed relied mainly on hydrothermal alteration minerals as temperature proxies. For a geothermal system to exist, the following conditions must be present; a heat source, recharge fluid, permeable formations and/or structures to allow water to percolate through and time for heat transfer from the hot intrusive to the water which is the media.

Occurrences of acidic and pantelleritic rock units on the surface and at shallow depths with comendites at deeper levels indicate a highly differentiated magma chamber source. Extrusions and intrusions of magma occur along the N-S structure and the ring structure; this resulted into the emplacement of a shallow heat source in form of brittle ductile plutonic bodies. The volcanicity in Olkaria is still active and is attributed to tectonics leading to increased activity in the area as evidenced by the recent Ololbotut eruption, which has been dated at 180 ± 50 yrs (Clarke *et al.* 1990). Due to these evidences the heat source in Olkaria area is a hot plutonic body below 6 km and this is corroborated by Seismic studies. According to (Simiyu *et al.* 1998) the presence of a semi molten magma bodies, whose depths to their roots are not known, have been determined by shear wave attenuation below the 6 km depth.

Evidence from alteration minerals show that actinolite mineral is encountered at a relatively shallower depth in well OW-710 (Olkaria Northeast field). The actinolite is an alteration mineral formed by contact metamorphism when a hot magmatic body intrudes the country rocks, baking the areas adjacent to it (aureole). Using this and the high calculated temperatures from fluid geochemistry, the Olkaria Northeast field therefore an upflow zone. The shallower hot body heats the fluids and flows in convectional cell manner, the fluids outflow to Olkaria East and Olkaria Domes. These outflow zones are characterized by relatively low temperatures inferred from the mineralogy and calculated temperature from fluid geothermometry. Olkaria West showed the lowest temperatures indicating that it is an inflow zone or a recharge area.

A conceptual model through A, B, C, and D (Figure 5.1, 5.2 and 5.3) therefore is been developed in this report. The model indicating that hot fluids ascend from Olkaria Northeast because of the high temperatures inferred by actinolite presence and high geothermetric temperatures. The high temperatures are due a hot Plutonic Body intruding the Northeast field as the heat source. The thermal fluids outflow laterally towards Olkaria East and Olkaria Domes area as inferred from moderate temperatures recorded from alteration and fluid geothermometry.

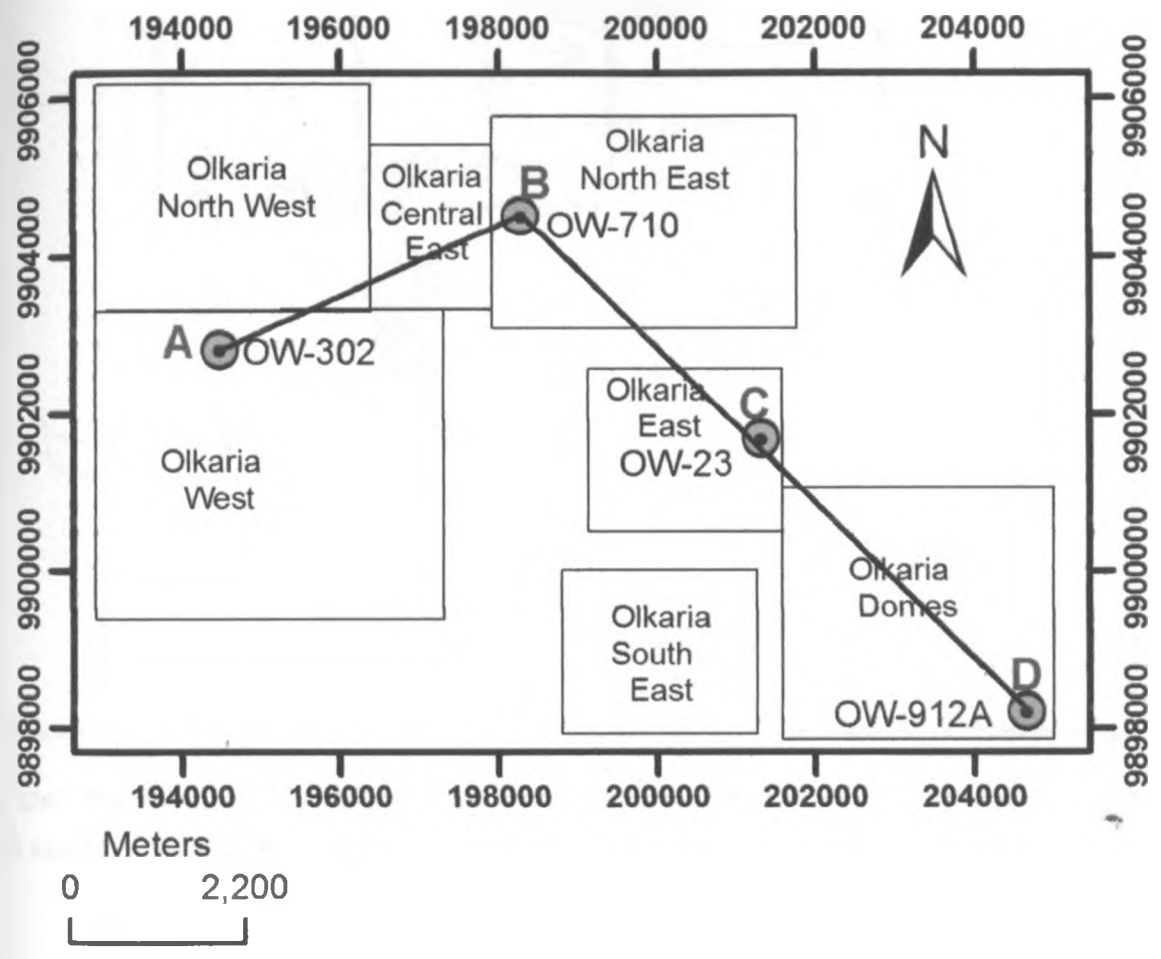


Figure 5.1: Cross-section line (A, B, C, and D)

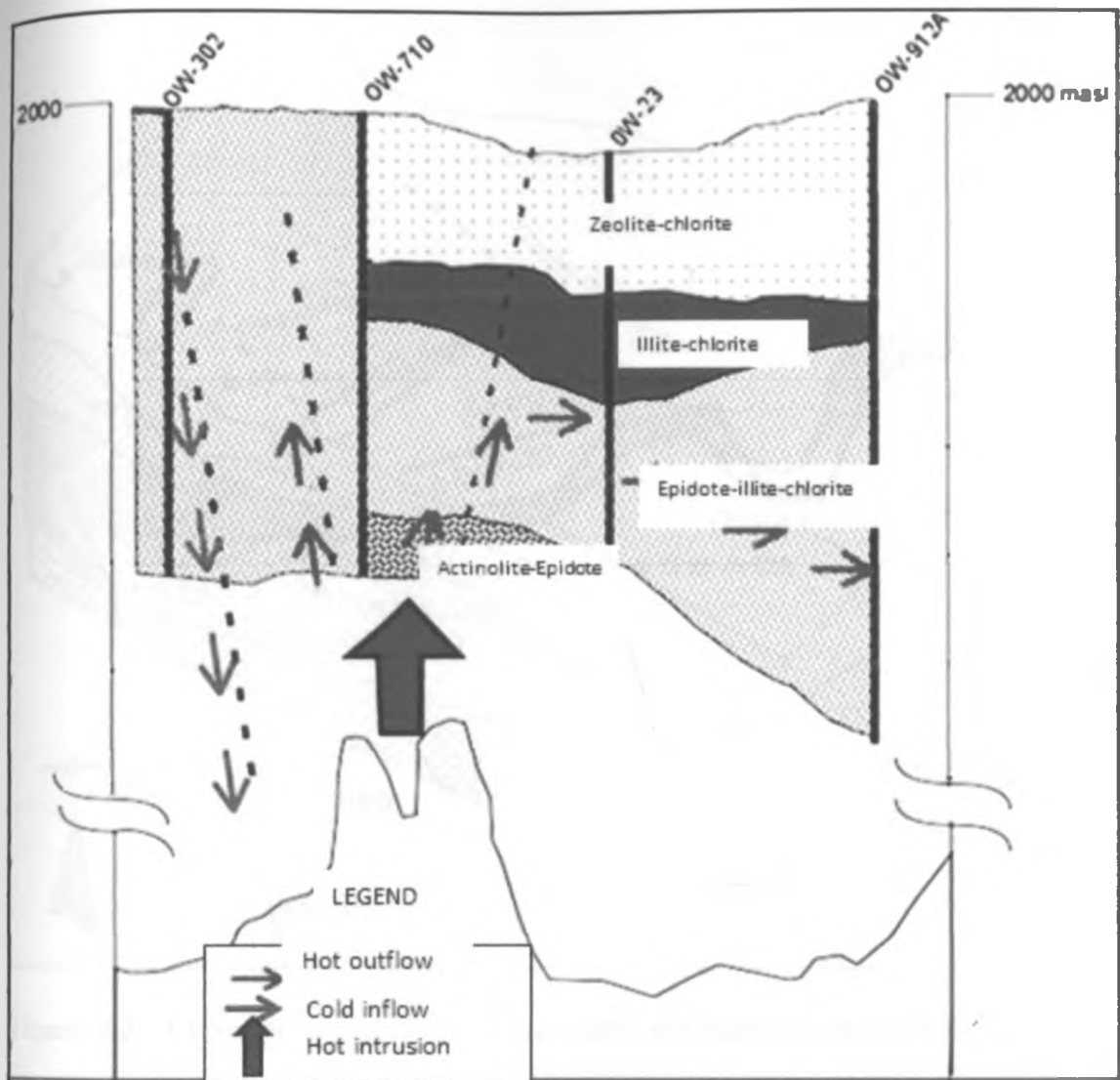


Figure 5.2: Integrated conceptual geothermal model using results of wells OW-710, OW-23 and OW-912A (NB/ Figure not drawn to scale).

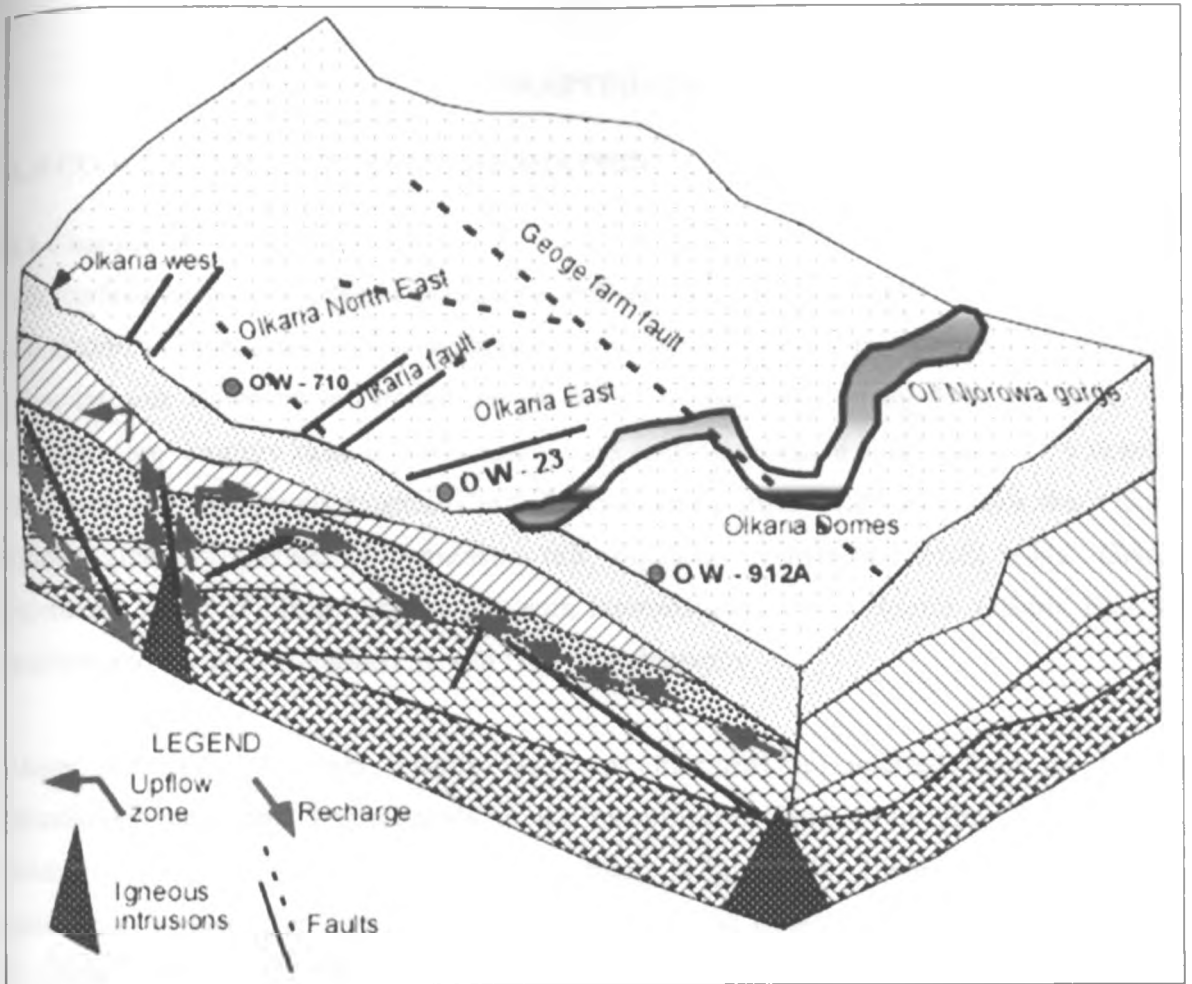


Figure 5.3: A three dimensional conceptual model of Olkaria geothermal field

CHAPTER SIX

6.0 CONCLUSION AND RECOMMENDATIONS

6.1 Conclusion

The surface geology of Olkaria geothermal field is dominated by basalts, trachytes, rhyolites, comendite and pyroclastics. Non-comenditic rhyolite extrusions of the area are confined to an irregular area which curves around the southwest on the shores of the Lake Naivasha. The rhyolites are younger than the comendites and may represent a later phase of volcanism involving common parent magma. The Lithostratigraphy from well logs reveals that Olkaria Domes area is composed of pyroclastic, tuff, rhyolites, trachyte and basalt while Olkaria Northeast are tuff layers and basalts with intercalations of pyroclastics. Olkaria East has trachyte and rhyolite as revealed by well OW-23 stratigraphy.

Major subsurface structures (mainly faults and fractures) are inferred from the loss of circulation/returns and displacements in the reconstructed Lithostratigraphy. The structures mainly occur around Olkaria East and Northeast (Figure 4.5). These areas are therefore permeable, making it possible for geothermal fluids to be transmitted, consequently, they are favorable areas for drilling. The chemical analysis of the rocks from Olkaria East, Olkaria Northeast and Olkaria Domes fields indicate that rocks from Olkaria East and Olkaria Northeast have compositions similar to those of Olkaria Domes generally with somewhat alkaline compositions. Based on classification in terms of Al_2O_3 and total iron (FeO), the Olkaria trachytes are pantelleritic with higher Al_2O_3 , Fe_2O_3 , CaO, and Na_2O . Major element variation plots for quartz trachytes and comendites show a linear trend for the variation of TiO_2 and Fe_2O_3 with SiO_2 .

Reservoir temperatures calculated using chemical geothermometers by K/Na ratio function by Arnorsson *et al.* (1983) indicate average temperature values of 258°C for the Olkaria West and 290°C for Olkaria Northeast. The quartz geothermometric function by Fournier and Potter (1982) is however much more reliable and indicates 255°C, 270°C and 240°C for Olkaria East, Olkaria Northeast and Olkaria Domes respectively. Olkaria Northeast is thus the hottest and

these results mirrors those inferred from alteration minerals (Figure 4.13). Therefore this validates and proves that geothermal fluids can be used as temperature proxies in geothermal conceptual modeling.

Based on hydrothermal alteration minerals assemblages in the three subfields, four alteration zones are recognized with a possibility of one or two sub-zones. The zones are: (1) The zeolite-chlorite zone; (2) The illite-chlorite zone; (3) The epidote-illite-chlorite zone; and 4) Actinolite-epidote zone. The zones infer temperatures of 0-225°C, 230-248°C, 248-300°C and >300°C, respectively. A conceptual model based upon thermal fluids and alteration mineral geothermometry suggests that Olkaria Northeast is the upflow with hot fluids ascending here and outflows laterally towards Olkaria East and Olkaria Domes area. A major intrusive in Northeast field inferred from young rocks in the area is the heat source, the ductile body transfers heat by conduction and eventually heats up the fluids forming thermal fluids.

6.2 Recommendations

1. Olkaria Northeast and to lesser extent Olkaria East should be given priority during production drilling since they are upflow areas as indicated by high temperatures.
2. Structural geology also indicates that the aforementioned subfields host the main subsurface structures that should be targeted during drilling.
3. Olkaria West should be a reinjection field since natural inflow is in that area.
4. Simulation studies using reservoir data should be done to refine the model developed in this project.
5. Reinjection index test should be carried out to map the extent of the reservoir in the Olkaria Northeast field.
6. More studies should be carried out incorporating more data from more wells in each field, this will help in making a more comprehensive model of the Olkaria geothermal field.

REFERENCES

- Ambusso, W.J., Ouma, P.A., 1991: Thermodynamic and permeability structure of Olkaria Northeast field. *Geothermal Resource Council Transactions*, 15, 237-242.
- Amorsson, S., Gunnlaugsson, E., Svarvarson, H., 1983: The chemistry of geothermal waters in Iceland III. Chemical geothermometry in geothermal investigations. *Geochemica Cosmochemica Acta*, 46, 1513-1532.
- Baker, B.H., Mohr, P.A., Williams, L.A.J., 1972: Geology of the eastern rift system of Africa. *Geological Society of America*, Special paper 136, 1-67.
- Baker, B.H., Williams, L.A.J., Miller, J.A., Fitch, F.J., 1971: Sequence and geochronology of the Kenya Rift volcanics. *Tectonophysics*, 11, 191-215.
- Baker, B.H., Wohlenberg, J., 1971: Structural evolution of the rift valley, *Nature*, 229, 538-542.
- Billings, M.P., 1972: Structural Geology 3rd edition, New Delhi, pp. 249-250.
- Black, S., Macdonald, R., Kelly, M.R., 1997: Crustal origin of per alkaline rhyolites from Kenya: evidence from U-series disequilibria and Th-isotopes. *Journal of Petrology*, 38, 277-297.
- Browne, P.R.L., 1981: Petrographic study of cuttings from drilled wells at the Olkaria Geothermal field, Kenya. Kenya Power Company.
- Browne, P.R.L., 1978: Hydrothermal alteration in active geothermal fields. *Annual Review Earth and Planetary Sciences*, 6, 229-250.
- Cathelineau, M., Oliver, R., Garfias, A., 1985: Mineralogy and distribution of hydrothermal mineral zones in Los Azufres (Mexico) geothermal field. *Geothermics*, 14, 49-57.
- Clarke, M. C. G., Woodhall, D. G., Allen, D., Darling, G., 1990: Geological, volcanological and hydrogeological controls of the occurrence of geothermal activity in the area surrounding Lake Naivasha. *Ministry of Energy, Nairobi, report 150*, 138 pp.
- Colin. H., Patrick, B., 2000: Mixed-layered clays in geothermal systems and their effectiveness as mineral geothermometers. Proceedings of World Geothermal Congress May-June 2000, Kyushu-Tohoku Japan, viewed 5th January 2012, <http://www.geothermal-energy.org>.

- Dunkley P.N Dunkley, P. N., Smith, M., Allen, D. J. and Darling, W. G., 1993. The geothermal activity and geology of Northern sector of the Kenya Rift Valley. *British geological survey research report*, 93, 1.
- Ferguson, G., Grasby, S.E., and Hindle, S.R., 2009: What do aqueous geothermometers really tell us? *Geofluids*, 9, 39-48.
- Fournier, R.O., 1997: Chemical geothermometers and mixing models for geothermal systems. *Geothermics*, 5, 41-50.
- Fournier, R.O., Potter, R.W., 1982: A revised and expanded silica (quartz) geothermometer. *Geothermal Resource Council Bulletin*, 11-10, 3-13.
- Fournier, R.O., 1979: A revised equation for the Na/K geothermometer. *Geothermal Resources Council Transactions*, 3, 221-224.
- Giggenbach, W.F., 1991: Chemical techniques in geothermal exploration; in applications of geochemistry in geothermal reservoir development. *Cosmochemica Acta*, pp. 119-144.
- Giggenbach, W.F., 1988: Geothermal solute equilibria, derivation of Na-K-Mg-Ca geothermometers. *Geochemica Cosmochemica Acta*, 5, 2749-2765.
- Kamunzu, A.B., Mohr, P., 1991: Magmatic evolution and petrogenesis in the East Africa Rift system. *Springer-Verlag*, 2, 85-136.
- Karingithi, C.W., 1999: Olkaria Domes geothermal field Kenya, geochemical model. Kengen, unpublished internal report
- Karingithi, C.W., Wambugu, J.M., 1997: Olkaria Geochemical Model. Kenya Power Company, unpublished internal report.
- Karingithi, C.W., 1996: Olkaria East Production Field geochemical report. Kenya Power Company, unpublished internal report.
- Karingithi, C.W., 1993: Olkaria East Production Field geochemical report. Kenya Power Company, unpublished internal report.
- Karingithi, C.W., 1992: Olkaria East Production Field geochemical report. Kenya Power Company, unpublished internal report.
- Lagat, J.K., 2004: Geology hydrothermal alteration minerals and fluid inclusions studies of Olkaria domes geothermal field, Kenya. M.Sc. thesis, University of Iceland. 79 pp.

- Macdonald, R., Bagiński, B., Leat, P.T., White, J.C., Dzierżanowski, P., 2011: Mineral stability in peralkaline silicic rocks: Information from trachytes of the Menengai volcano, Kenya. *Journal of Petrology and geochemistry*, 125, 553–568.
- Macdonald, R., Davies, G.R., Bliss, C.M., Leat, P.T., Bailey, D.K., Smith, R.L., 1987: Geochemistry of high silica per alkaline rhyolites, Naivasha, Kenya rift valley. *Journal of* 28, 979-1008.
- Macdonald, R., 1974: Nomenclature and petrochemistry of the peralkaline oversaturated extrusive rocks. *Bulletin of Volcanology*, 38, 498-516.
- Muchemi G.G., 2000: Conceptualized model of Olkaria geothermal field, Kengen, 13 pp.
- Mungania, J., 1992: Preliminary field report on geology of Olkaria volcanic complex with emphasis on Domes area field investigations. Kenya Power Company, 38 pp.
- Ogoso-Odongo, M.E., 1986: Geology of Olkaria geothermal field. *Geothermics*, 15, 741-748.
- Omenda P.A 1998: The geology and structural controls of the Olkaria geothermal system Kenya. *Geothermics* 27, 55-755.
- Omenda, P.A., 2000: Anatectic origin for Comendite in Olkaria geothermal field, Kenya Rift; Geochemical evidence for syenitic protolith. *African Journal of Science and Technology. Science and Engineering Series*, 1, 39-47.
- Naylor, W. I., 1972: The geology of the Eburru and Olkaria geothermal projects. Geothermal Resource Exploration Prospects, viewed 18th February 2010, <http://www.os.is/gogn/unu-gtp-sc/UNU-GTP-SC-10-0102>.
- Ndombi, J.M., 1981: The structure of the shallow crust beneath the Olkaria geothermal field, Kenya, deduced from gravity studies. *Journal of Volcanology and Geothermal Research*, 9, 237-251.
- Utami, P., Browne, P.R.L., Simmons, S.F., Suroto, J., 2005: Hydrothermal alteration mineralogy of the Lahenndong geothermal system north Sulawesi, Paper presented at the 27th geothermal workshop 2005, New Zealand, viewed 18th February 2008, <http://www.science.auckland.ac.nz/uoa>.

- Reyes, A.G., 1990: Petrology of Philippine geothermal system and the application of alteration Mineralogy to their assessment. *Journal of Volcanology and Geothermal Research*, 43, 279-304.
- Sarolkar. p., 2000: Assessment of Tatapani geothermal field, India, based on hydrothermal mineral assemblage. Proceedings of World Geothermal Congress June 2000, Kyushu-Tohoku Japan, viewed 5th January 2012, <http://www.geothermal-energy.org>.
- Simiyu, S.M., Oduong, E.O and Mboya, T.K., 1998: Shear wave attenuation beneath the Olkaria volcanic field. Naivasha Kenya, KenGen.
- Simiyu, S.M., Omenda, P.A., Antony, E.Y., Keller, G.R., 1995: Geophysical and geological evidence for the occurrence of shallow intrusion in Naivasha sub-basin of the Kenya rift. Proceedings of AGU Fall 1995, viewed, 5th January 2010, <http://www.agu.org/meetings>.
- Smith, M., 1994: Stratigraphy and structural constrains on mechanisms of active rifting in the Gregory Rift, Kenya. In: Prodehl, C., Keller, G.R., Khan, M.A. (ed.), Crustal and upper mantle structures of the Kenya rift. *Tectonophysics*, 236, 3-2.
- Smith, M and Mosley, P., 1993: Crustal heterogeneity and basement influence on the development of the Kenya rift, East Africa. *Tectonics*, 12, 591-606.
- Virkir, S., 1976: Feasibility report for the Olkaria Geothermal Project. Nairobi Kenya, United Nations.
- Thompson, A.D and Dodson, R: 1963. Geology of the Naivasha Area. Geological Survey of Kenya, Nairobi, Kenya, Government Printer.
- Tiainen, S., King,H., Cubitt,C., Karalaus,E., Prater,T., Willis,B., 2002: A new approach to reservoir description and characterization. Examples from copper basin, Australia. Proceedings of Australian petroleum products and exploration association conference Adelaide Australia, viewed 5th January 2012, [http:// www.eps.mq.edu.au](http://www.eps.mq.edu.au).
- Virkir Consulting Group., 1980: Geothermal development at Olkaria. Naivasha Kenya, Kengen.
- Wambugu, J.M., 1995: Geochemical up-date of Olkaria West geothermal Field. Naivasha Kenya, Kengen.

APPENDIX IA: Preparation of samples for clay analysis

1. Into a clean test tube place approximately two spoonfuls of drill cuttings. Wash the cuttings to remove the dust with distilled water and fill the tube to approximately two-third full with distilled water. Place the tubes in a mechanical shaker for 4-6 hours depending on the intensity of alteration of the cuttings.

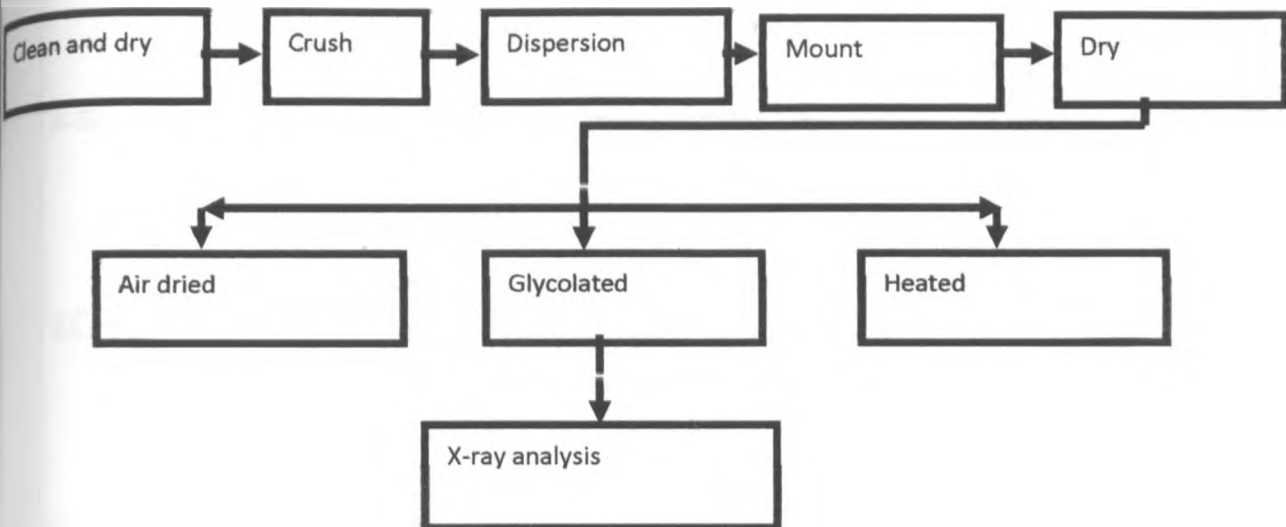
2. Allow the particles to settle for 1-2 hours, until those particles less than approximately 4 Å are left in suspension. Pipette a few millilitres from each tube and place approximately 10 drops on a labeled glass plate, not making the film thick. Make a duplicate of each sample and let them dry at room temperature overnight.

3. Place one sample at the desiccators containing glycol ($C_2H_6O_2$) solution and the other in a set of desiccator containing hydrated calcium chloride ($CaCl_2 \cdot H_2O$). Store it at room temperature for at least 24 hours. Thicker samples need more time at least 48 hours.

4. Run both sets of samples in the range 2-14° at intervals of 0.02°, 2θ for a time of 1 second on XRD machine.

5. Place one set of samples (usually the glycolated one) on an asbestos plate and insert in a preheated oven. Heat the samples at 500-550°C for one hour making sure the oven temperatures do not exceed 600°C. When the samples have cooled, run them in the range 2-14° on the XRD machine.

APPENDIX IB: A flow chart on procedure for XRD analysis



APPENDIX II: Well logging data of OW-912A based on binocular microscope analysis

STRATIGRAPHY OF WELL 912A			
Depth	Rock description	Rock type	hydrothermal alteration minerals
0-50	Brownish, light grey, unconsolidated rock cuttings consisting of soils, pumice, obsidian, quartz and glass fragments	Pyroclastic	Oxides Clays
50-72	Greenish to greenish grey, fine grained lava. Porphyritic with quartz and feldspars and moderately altered.	Rhyolite	Oxides Clays
72-170	Brownish to reddish brown fine grained lava, porphyritic with quartz and feldspars it is moderately to highly oxidized. Pyrite disseminated in ground mass, vein filling with pyrite.	Rhyolite	Oxides Clays
170-190	Brownish grey fine grained almost fresh lava it is porphyritic with quartz and feldspars	Rhyolite	Oxides Clays
190-252	Grey almost fresh lava. It is fine grained and crystalline it is porphyritic with quartz and feldspars it is weakly altered.	Rhyolite	Oxides Clays
252-287	Greenish grey fine grained quartz and feldspars weakly porphyritic lava. It's moderately altered to	Rhyolite	Oxides Clays

	brownish and greenish.		
287-310	Light grey fine grained quartz and feldspars phytic lava. it is weakly altered to brownish clay	Rhyolite	Oxides Clays
310-342	Greenish grey to greenish grey fine grained quartz rich lava. Moderately altered.	Rhyolite	Oxides Clays
342-360	Light grey to greenish grey fine grained feldspar rich phytic lava it is moderately altered and appears fractured	Trachyte	Oxides Clays Pyrite
360-442	Loss of returns/ circulation	-	-
442-450	Light grey weakly porphyritic lava with feldspars. it is fine grained and moderately altered to clays. It's also bleached	Trachyte	Oxides Clays Pyrite
450-458	Loss of returns/ circulation	-	-
458-460	Light grey weakly porphyritic lava with feldspars. It is fine grained and moderately altered to clays. It's also bleached.	Trachyte	Oxides Clays Pyrites
460-488	Loss of returns/ circulation		
488-514	Light grey fine grained quartz and feldspar rich lava. It is silicic, moderately altered and porphyritic.	Rhyolite	Clay Oxides pyrite
514-522	Loss of returns/ circulation	-	-
522-580	Light grey fine grained quartz and feldspar rich lava. It is silicic,	Rhyolite	Clay Oxides

	moderately altered and porphyritic.		pyrite calcite
580-584	Light grey fine grained feldspar rich lava. It is moderately altered and has some green coloration.	Trachyte	Clays Pyrite Chlorite calcite
584-586	Loss of returns/circulation	-	-
586-588	Light grey to greenish grey fine grained feldspar rich phyric lava. Has veins filled with quartz. Also pyrite is disseminated in the groundmass. It is moderately altered and appears fractured.	Trachyte	Clays pyrite Chlorite calcite
588-654	Loss of returns/circulation	-	-
654-662	Light grey to greenish grey fine grained feldspar rich phyric lava. Has veins filled with quartz. Also pyrite is disseminated in the groundmass. It is moderately altered and appears fractured.	Trachyte	Clays Pyrite Quartz Chlorite calcite
662-666	Loss of returns/circulation	-	-
666-668	Light grey to greenish grey fine grained feldspar rich phyric lava. Has veins filled with quartz. Also pyrite is disseminated in the groundmass. It is moderately altered and appears fractured.	Trachyte	Pyrite Clays Quartz Chlorite
668-670	Loss of returns/circulation	-	-
670-680	Light grey to greyish grey fine feldspar rich phyric lava. Has veins filled within quartz. Also pyrite is	Trachyte	Oxides Clays Pyrite

	disseminated in the groundmass. It's moderately altered and appears fractured.		Quartz
680-682	Loss of returns/circulation	-	-
682-684	Light grey to greenish grey fine grained feldspar rich phytic lava. Has veins filled with quartz .Also pyrite is disseminated in groundmass .Its moderately altered and appears fractured.	Trachyte	Oxides Clays Pyrites Quartz
684-790	Loss of returns/circulation	-	-
790-792	Light grey to grey fine grained quartz and feldspar phytic lava. It's moderately altered to greenish and brownish clays.	Trachyte	Clays Chlorite Pyrite Epidote
792-846	Loss of returns/circulation	-	-
940-944	Grey to grayish green fine grained lava. It's porphyritic with feldspars. It also has veins filled with quartz .It is fractured and shows moderate to high intensity of alteration.	Trachyte	Clays Chlorite Pyrite Epidote Quartz
944-990	Dark grey feldspar phytic lava. It is highly porphyritic and has reddish brown tinges on the groundmass. It also has abundant calcite .It appears fractured and moderately altered to brownish and greenish clays.	Basalt	Clays Chlorite Pyrite Epidote
990-1012	Grey to brownish grey feldspar phytic lava. It is moderately to highly porphyritic .It shows flow banding, veined and fractured. It's	Basalt	Clays Chlorite Pyrite Epidote

	moderately altered to brownish, greenish and reddish brown.		
1012-1018	Greyish green fine feldspar phyric lava. It is moderately porphyritic and veined. It's also chloritized at some depths. It's moderately altered to greenish and whitish clays.	Trachyte	Clays Chlorite Pyrite Epidote Calcite
1018-1040	Brownish grey fine grained moderately altered lava. It is moderately too high porphyritic. It has reddish brown tinges on the groundmass. It is also veined and fractured	Basalt	Clays Chlorite Pyrite Epidote (abundant) Calcite
1040-1070	Dark grey moderately porphyritic with feldspars lava. It has reddish brown tinges on the matrix. It is also veined and appears fractured.	Basalt	Clays Chlorite Pyrite Epidote (abundant) calcite
1142-1152	Grayish to grayish green feldspar phyric lava. It is weakly porphyritic and slightly chloritized. It is also veined.	Trachyte	Clays Chlorite Pyrite Epidote (abundant) quartz
1152-1162	Light brown brownish grey lava. It is porphyritic with feldspar. It is also fractured. Moderately altered to clays	Trachyte	Clays Chlorite Pyrite Epidote (abundant)
1162-1174	Greyish to greyish green feldspar	Trachyte	Clays

	phyric lava. It is weakly porphyritic and slightly chloritized. It is also veined.		Chlorite Pyrite Epidote (abundant)
1174-1178	Grey to grayish brown feldspar phyric lava. It is fine grained and has reddish brown alterations.	Trachyte	Clays Chlorite Pyrite Epidote (abundant)
1178-1180	Light grey to grey, quartz phyric lava. It is fine grained and crystalline. It also shows flow banding and moderately altered to brownish and greenish clays.	Rhyolite	Clays Chlorite Pyrite Epidote (abundant)
1180-1194	Loss of returns/circulation		
1194-1214	Light grey to grey fine grained feldspar phyric lava. It shows flow banding and also veined it is weakly to moderately altered	Trachyte	Clays Chlorite Pyrite
1214-1194	Light grey to greyish feldspar rich lava. It is fine grained, veined and fractured. Shows moderate intensity of alteration.	Trachyte	Clays Chlorite Epidote Quartz
1412-1416	Light grey to bluish grey highly porphyritic with feldspar. It shows flow banding, veined and appears fractured. It is moderately altered to clays	Trachyte	Clays Chlorite Epidote pyrite
1416-1422	Pale green to light weakly porphyritic lava. It is rich in fields and appears fractured. It also has	Trachyte	Clays Chlorite Epidote

	brownish alteration		
1422-1438	Grayish to greenish grey fine grained lava. It is weakly porphyritic and highly altered.	Trachyte	Clays Chlorite Epidote
1442-1456	Brownish grey, bluish grey weakly to moderately porphyritic with feldspar. It is fracture and shows moderately to high intensity of alteration	Trachyte	Clays Chlorite Epidote
1456-1468	Brownish to reddish brown fine grained vesicular lava. It appears light weight and moderately altered to white clays	Tuff	Clays Chlorite Epidote
1462-1472	Light grey to bluish grey fine grained lava. It is porphyritic with feldspar. Moderately altered to bluish and brownish clays	Trachyte	Clays Chlorite Epidote pyrite
1472-1486	Light grey to brownish grey fine grained feldspar phytic lava. It is veined and highly altered to reddish brown	Trachyte	Clays Chlorite Epidote pyrite
1486-1490	Greenish grey fine grained porphyritic lava. It is moderately altered and appears fractured.	Trachyte	Clays Chlorite Epidote pyrite
1490-1540	Light grey to brownish grey phytic lava. It has quartz and feldspar rich, moderately altered and appears fractured.	Rhyolite	Clays Chlorite Epidote pyrite

1540-1546	Greenish grey porphyritic rock. It is moderately altered and appears fractured.	Trachyte	Clays Chlorite Epidote
1546-1588	Light brown to light grey fine grained porphyritic lava. It is moderately altered, fractured and veined.	Trachyte	Clays Chlorite Epidote
1588-1618	Light grey, grey, greenish brown highly porphyritic with quartz. It is crystalline and fractured. Has veins filled with black mineral. Moderately altered to clays.	Rhyolite	Clays Chlorite Epidote
1618-1680	Grey fine grained weakly to moderately porphyritic with feldspars. It is fractured and almost fresh to weakly altered.	Trachyte	Clays Epidote
1660-1698	Light grey fine grained crystalline lava. It is porphyritic with quartz and feldspar. It has reddish brown alterations. It is also fractured and shows moderate to high intensity of alteration	Rhyolite	Clay Chlorite Epidote Pyrite Quartz
1698-1728	Light grayish to grayish fine grained feldspar phyric lava. Shows shiny appearance on the surface. It is moderately altered and has veins filled with quartz light grey, grayish fine	Trachyte	Clay Chlorite Epidote Pyrite
1728-1760	Light grey fine grained lava. It is crystalline and moderately porphyritic with quartz. It is	Rhyolite	Clay Chlorite Epidote

	fractured and weakly altered.		Pyrite Quartz
1760-1776	Brown to brownish grey weakly porphyritic with feldspar lava. It is fine grained and highly altered to greenish and whitish clays. It is also veined and fractured.	Trachyte	Clay Chlorite Epidote Quartz
1776-1784	Light grey fine grained feldspar porphyritic lava. It is fractured and also moderately altered	Trachyte	Clays Chlorite Epidote
1784-1794	Grayish to grayish brown fine grained phytic lava. It is veined, fractured and moderately altered to clays	Trachyte	Clays Chlorite Epidote
1828-1842	Dark grey to grey feldspar phytic lava. It is fine gained and moderately to highly porphyritic. Highly altered to greenish, brownish and whitish clays.	Trachyte	Clay Chlorite Epidote Quartz
1842-1850	Light to whitish green bleached rock. It is weakly porphyritic with feldspar. It is also highly altered.		
2100-2178	Brownish grey, fine grained weakly porphyritic. It is fractured and has quartz veins and moderately to highly altered. Also has reddish brown tinges and is shinny on the surface.	Trachyte	Epidote Clays Biotite Quartz Chlorite
2178-2212	Greenish grey fine grained phytic lava with feldspar. It is moderately	Trachyte	Epidote Clays

	altered and has reddish brown alterations. Also appears fractured.		Quartz Chlorite
2212-2300	Brownish grey moderately porphyritic lava with feldspars. It is moderately to highly altered and appears fractured.	Trachyte	Epidote Clays Quartz Chlorite
2300-2356	Light grey, light brown fine grained quartz and feldspars porphyritic lava. It is moderately altered to clays.	Trachyte	Clays Chlorite Epidote
2356-2372	Brownish grey moderately porphyritic lava with feldspars. Moderately altered to brownish clays and appears fractured	Trachyte	Clays Chlorite Epidote
2372-2438	Light brown fine grained feldspar rich lava. It has veins filled with quartz and moderately altered to clays.	Trachyte	Clays Chlorite Epidote
2438-2458	Light grey to greyish feldspar rich lava. It is fine grained, veined and fractured. Shows moderate intensity of alteration.	Trachyte	Clays Chlorite Epidote Quartz
2458-2468	Light grey to greyish feldspar rich lava. It is fine grained, veined and fractured. Shows moderate intensity of alteration.	Trachyte	Clays Chlorite Epidote Quartz
2468-2504	Light grey to grey fine grained phytic lava. It is veined, fractured and flow banding is evident and it's moderately altered.	Trachyte	Epidote Clays Quartz Chlorite
2504-2514	Grey to brownish grey fine grained	Trachyte	Epidote

	phyric lava. It's moderately to highly altered to brownish clays and appears fractured.		Clays Chlorite
2514-2556	Greyish fine grained feldspar and quartz rich crystalline lava. It is moderately to highly altered and it's also moderately porphyritic.	Rhyolite	Epidote Clays Chlorite
2556-2606	Light grey to greyish fine grained feldspar rich lava. It is moderately altered to brownish. It is also veined and fractured.	Trachyte	Epidote Clays Chlorite Quartz
2606-2608	Loss of returns/circulation	-	-
2608-2624	Light grey to greyish fine grained feldspar rich lava. It is moderately altered to brownish. It is also veined and fractured.	Trachyte	Epidote Clays Chlorite Quartz
2624-2626	Loss of returns/circulation	-	-
2626-2658	Light grey to greyish fine grained feldspar rich lava. It is moderately altered to brownish. It is also veined and fractured.	Trachyte	Epidote Clays Chlorite Quartz
2658-2680	Brownish grey to grey fine grained phyric lava. It is moderately altered to brownish clays and it appears fractured.	Trachyte	Epidote Clays Chlorite Quartz
2680-2730	Light brown light feldspar rich moderately porphyritic lava. It shows moderate to high intensity of alteration	Trachyte	Epidote Clays Chlorite
2730-2742	Loss of returns/circulation	-	-
2742-2770	Light grey feldspar rich moderately	Trachyte	Epidote

	porphyritic lava. It is crystalline and shows moderate to high intensity of alteration to brownish clays.		Clays Chlorite Pyrite
2770-2786	Loss of returns/circulation	-	-
2786-2794	Light grey to light brown fine grained porphyritic lava feldspar. It is moderately altered and also appears fractured.	Trachyte	Epidote Clays Chlorite Pyrite
2794-2816	Light grey to brownish grey fine grained highly porphyritic with black phenocrysts on feldspar matrix. It is silicic and shows moderate to high intensity of alteration to clays. It has reddish brown tinges on the groundmass.	Trachyte	Epidote Clays Chlorite Pyrite
2816-2832	Brownish grey to grey fine grained lava. It is fine grained and fractured. It is fine grained and fractured. It is porphyritic with feldspars. It also shows flow banding. It is moderately altered to clays.	Trachyte	Epidote Clays Chlorite Pyrite
2832-2840	Bluish to bluish grey fine grained feldspar phyric lava. It is silicic and highly altered to clays.	Trachyte	Epidote Clays
2840-2856	Brownish grey fine grained lava. Shows flow banding and fracturing .Its moderately altered to brownish and bluish clays	Trachyte	Epidote Clays Chlorite
2856-2864	Grey fine grained moderately to highly altered lava. Shows flow	Trachyte	Epidote Clays

	banding and it's also silicic and altered to brownish.		Chlorite
2864-2874	Loss of returns/circulation	-	-
2874-2884	Greyish to bluish fine grained feldspar rich moderately porphyritic lava. It is moderately altered to bluish clays.	Trachyte	Epidote Clays Chlorite
2884-2958	Light brown to brownish grey grained phyric lava. It shows moderate to high intensity of alteration to bluish and brownish clays.	Trachyte	Epidote Clays Chlorite
2958-2990	Light grey light brown moderately porphyritic lava with feldspars. It is moderately altered and has reddish brown tinges on the matrix.	Trachyte	Epidote Clays Chlorite

APPENDIX III: Clay analysis and interpretation

Ref ID	Air dried D-spacing (intensity)	Glycolated D-spacing (intensity)	Heated D-spacing (intensity)	Interpretation
50-60	7.19(60), 10.14(50)	7.19(38), 10.06(44)	Kaolinite, illite
78-80	7.12(8)	7.03(17)	7.02(6), 7.19(19)	illite
98-100	7.17(4), 10.11(31)	7.16(30), 10.1(30)	7.10(9), 10.01(58)	Illite, kaolinite
316-320	7.07(48), 10.32(100)	7.09(42), 10.09(10)	10.10(100)	Illite, kaolinite
358-360	7.01(91), 9.91(100)	7.02(99), 10.19(29)	10.09(100)	Kaolinite, illite
378-380	7.10(21), 10.19(12)	7.12(18)	7.15(7), 10.13(13)	Kaolinite, illite
400-402	7.13(46), 10.05(36)	7.12(56), 9.97(56)	7.08(56), 7.18(38)	Illite, kaolinite
416-424	7.40(14), 10.30(34)	7.41(100), 10.00(40)	7.16(5), 10.14(100)	Illite, kaolinite
438-440	14.00(100)	7.06(97), 10.27(99)	7.39(15), 10.10(100)	illite, chlorite
458-460	7.05(100), 15.06(23)	7.34(77), 17.01(38)	7.32(42), 10.09(25)	Chlorite, illite
478-480	7.07(64), 10.06(23)	7.19(47), 10.009(16)	7.30(180), 10.10(45)	Chlorite, illite
518-520	7.11(100), 10.42(19)	10.3(12), 14.04(12)	7.36(32), 10.03(100)	Chlorite, illite
538-540	7.11(100)	7.10(100), 7.38(29)	7.01(29), 7.39(100)	Chlorite
558-560	7.07(100), 10.14(9)	7.41(100), 10.07(21)	Chlorite, illite
578-580	7.07(46), 10.13(100)	7.07(30), 9.91(100)	7.01(95), 10.03(9100)	Chlorite, illite
638-640	7.10(100), 10.16(10)	10.02(7), 14.2(49)	7.16(40), 10.03(15)	Chlorite, illite
656-660	7.12(100), 10.29(11)	7.15(100), 10.14(7)	7.31(46), 10.05(22)	Chlorite, illite
698-700	10.09(9), 14.47(41)	10.5(10), 14.77(37)	7.11(33), 14.19(100)	Chlorite, illite
730-732	7.06(100), 10.30(27)	7.10(99), 10.00(19)	7.24(38), 9.87(38)	Chlorite, illite
738-740	7.10(100), 10.16(33)	7.05(67), 10.01(100)	Chlorite, illite
742-744	7.07(100), 10.13(10)	7.11(99), 14.03(36)	Chlorite, illite
754-756	7.07(100), 10.03(16)	7.26(99), 10.22(24)	7.01(24), 9.97(44)	Chlorite, illite

778-780	7.07(100), 9.97(10)	7.11(100), 9.94(19)	7.06(26), 10.07(27)	Chlorite, illite,
838-842	7.07(100), 10.09(97)	7.08(99), 14.10(38)	7.29(10), 14.02(38)	Chlorite, illite
878-880	7.09(100), 10.14(65)	7.13(99), 10.03(59)	7.12(67), 10.02(100)	Chlorite, illite
918-920	7.06(100), 10.09(77)	7.05(100), 9.98(64)	7.27(30), 10.03(100)	Chlorite, illite Chlorite/illite
958-960	7.10(100), 10.14(10)	7.06(100), 17.54(5)	7.21(39), 9.98(89)	Chlorite, illite, Smectite
978-980	7.11(100), 9.80(7)	7.08(100), 9.97(7)	12.288(100)	Chlorite, illite
998-1000	7.17(100), 10.12(17)	7.14(99), 10.07(13)	7.02(38), 9.99(100)	Chlorite/illite, smectite
1018-1020	7.11(100), 10.19(5)	7.12(99), 10.17(23)	7.09(43), 10.01(9)	Chlorite, illite, smectite
1082-1084	7.10(100), 10.11(26)	7.12(99), 10.17(23)	10.01(93), 14.14(43)	Illite/Chlorite
1098-1100	7.05(100), 10.24(19)	7.18(99), 10.26(30)	7.27(71), 9.90(88)	Chlorite, illite
1120-1124	7.08(100), 10.04(24)	7.05(100), 17.36(9)	7.04(75), 9.98(72)	Chlorite, illite
1140-1142	7.09(100), 10.22(4)	7.14.11(26), 16.7(4)	7.14(38), 10.21(12)	Chlorite, illite, smectite Illite/Chlorite.
1210-1212	7.09(100), 4.13(36)	7.07(100), 12.28(7)	7.12(28), 12.35(26)	Chlorite, illite, Illite/Chlorite

1238-1240	7.06(100), 9.92(25)	7.08(99), 14.08(31)	10.04(95), 14.19(100)	Chlorite, illite, illite/Chlorite (?)
1254-1256	7.09(100), 14.05(19)	7.08(100), 17.08(3)	7.28(100), 14.17(29)	Chlorite, illite, smectite
1338-1340	7.10(100), 14.13(11)	7.07(100)	Chlorite
1356-1360	7.10(100), 10.07(34)	7.07(99), 11.88(18)	7.08(32), 10.06(97)	Chlorite, illite, illite/Chlorite
1380-1382	7.08(100), 11.80(12)	7.08(100), 14.21(7)	7.02(93), 12.02(100)	Chlorite, illite/Chlorite
1398-1400	10.02(6), 14.04(16)	7.07(99), 12.14(35)	7.05(21), 14.12(38)	Chlorite, illite, illite/Chlorite
1420-1422	7.07(100), 14.17(3)	7.05(100)	7.34(100)	Chlorite.
1490-1494	7.10(100), 9.95(13)	7.08(100), 10.04(9)	7.09(13), 9.89(100)	Chlorite, illite, illite/Chlorite
1518-1520	7.08(100), 10.15(9)	7.08(100), 10.04(6)	7.11(100), 10.04(38)	Chlorite, illite, (minor)
1538-1540	7.16(100), 10.09(9)	7.07(100), 10.29(9)	7.09(48), 10.09(34)	Chlorite, illite,
1558-1560	10.02(40), 15.06(24)	7.12(100), 10.46(9)	7.18(52), 10.03(43)	Chlorite, illite, smectite illite/Chlorite.
1588-1592	10.15(28), 14.07(63)	7.10(100), 7.10(5)	7.01(17), 14.17(99)	Chlorite, illite, smectite illite/Chlorite.
1616-1620	7.07(31), 10.08(51)	7.15(97), 10.13(90)	7.32(41), 9.96(100)	Chlorite, illite, illite/Chlorite.
1702-1706	7.07(100)	7.08(100), 14.15(12)	Chlorite,
1716-1718	7.09(100), 10.10(40)	7.07(99), 10.09(23)	7.07(31), 9.94(100)	Chlorite, illite. Illite/Chlorite.

1718-1720	7.11(25), 10.05(34)	10.05(44), 12.1(99)	9.90(98), 14.03(55)	Chlorite, illite. Illite/Chlorite.
1754-1756	7.08(100), 10.09(95)	7.10(97), 11.92(97)	7.04(16), 14.12(14)	Chlorite, illite. Illite/Chlorite.
1758-1760	7.08(100), 14.13(9)	7.11(100), 14.1(10)	7.21(100)	Chlorite,
1808-1812	10.27(22), 14.35(20)	7.10(100), 10.7(24)	7.01(6), 7.30(34)	Chlorite, illite.
1828-1832	10.15(20), 14.16(24)	7.06(100), 9.99(18)	7.18(100), 9.92(100)	Chlorite, illite.
1836-1840	7.15(100), 14.36(29)	7.14(99), 12.58(42)	7.29(10), 10.04(85)	Chlorite, illite. illite/Chlorite
1842-1844	7.08(52), 10.07(100)	7.07(56), 10.01(99)	7.09(7), 9.91(100)	Chlorite, illite. illite/Chlorite
1854-1856	7.12(100), 14.18(45)	7.13(100), 14.20(9)	10.15(13), 14.10(50)	Chlorite, illite.
1876-1880	7.16(10), 10.14(100)	7.00(20), 10.07(99)	7.11(14), 9.91(36)	Chlorite, illite. illite/Chlorite
1938-1940	7.11(95), 11.93(100)	7.15(10), 12.04(99)	7.07(5), 12.17(100)	Chlorite, illite. illite/Chlorite